Efficient Estimation of Nonlinear DSGE Models

Eva F. Janssens[†] and Sean McCrary[‡]

March, 2026

Most Recent Version

Abstract

This paper introduces a computationally efficient method for full-information estimation of nonlinear Dynamic Stochastic General Equilibrium (DSGE) models. In contrast to the traditional approach of treating model solution and filtering as two separate and potentially computationally intensive steps, we integrate the solution into the filtering procedure. The method computes a sequence of local linear solutions at the best forecast of the current state, yielding a time-varying linear state-space system for likelihood evaluation via the Kalman filter. The method captures nonlinear dynamics with high accuracy while avoiding global solution methods and nonlinear filtering, resulting in computational gains of several orders of magnitude. We benchmark the approach on canonical labor search and New Keynesian (NK) models. Applied to an NK model with labor market frictions, the method shows that these frictions generate state-dependent monetary policy transmission consistent with empirical evidence from local projections. The framework extends to models with stochastic volatility, regime switching, and heterogeneous agents.

Keywords: Bayesian inference, nonlinear filtering, computational methods

JEL classification codes: C63, C68, C32, E32, E52, J64

* Acknowledgements: We are grateful for Hilde Bjornland's discussion at Midwest Econometrics' mentoring meeting, and for the helpful comments of Ryan Michaels, Frank Schorfheide, Mikkel Plagborg-Møller, Marco del Negro, Adam McCloskey, Jean-Jacques Forneron and Kaspar Wüthrich, seminar, brown-bag, and conferences participants at UNC, OSU, Richmond Fed, NY Fed, SED, SEA, IAAE, Midwest Macro, Midwest Econometrics, and T2M. Part of this paper was earlier presented under the name "Unemployment and the State-Dependent Effects of Monetary Policy". Any errors are our own.

Contact information:
† Eva F. Janssens: University of Michigan, Department of Economics. evafj@umich.edu
‡ Sean McCrary: Ohio State University, Department of Economics. mccrary.65@osu.edu

This repository contains example code for several of the applications in this paper.

1 Introduction

Nonlinearities play a fundamental role in macroeconomic dynamics, and a growing empirical literature underscores their importance.[1] While macroeconomic models often feature such nonlinearities, whether they affect model predictions depends on the choice of solution and estimation method. Global solution methods combined with nonlinear filters are the most accurate way to solve and estimate such nonlinear models, but their computational cost quickly becomes prohibitive: estimation can take days, weeks, or months.[2]

The methodological contribution of this paper is a computationally efficient and broadly applicable approach to full-information estimation of nonlinear Dynamic Stochastic General Equilibrium (DSGE) models. Traditional estimation methods treat model solution and likelihood evaluation (using a filter) as two separate steps. Instead, our method characterizes the solution *within* the filtering procedure. The approach builds on the observation that even highly nonlinear models exhibit local behavior that can be well approximated by linear functions, but nonlinearity implies that these functions vary across the state space. The main idea is that, for estimation, an accurate characterization of nonlinear model dynamics can be obtained by repeatedly solving for such local approximations in the regions of the state space where the data indicates the economy is most likely to be.

Concretely, the method constructs a dynamic sequence of local linear solutions around the best forecast of the current state, and embeds the resulting policy rules in a time-varying linear state-space system. Each local solution is fast to compute and accurate in a neighborhood of the current state. The dynamic implementation of local linear methods preserves nonlinearities such as state dependence and, despite the policy functions being linear, yields solutions that are not certainty equivalent. The linear state-space form enables likelihood evaluation via the time-varying Kalman filter, eliminating the need for costly nonlinear filters. Theoretically and through simulation, we show that the proposed procedure closely approximates the object that would arise if the extended Kalman filter could be applied to the

[1] For example, Stock and Watson (2020); Benigno and Eggertsson (2024); Gitti (2024) examine nonlinearities in the Phillips curve; Tenreyro and Thwaites (2016) and Barnichon et al. (2022) analyzes state and sign dependence in the transmission of economic shocks, respectively.

[2] For example, in Gust et al. (2017), a single solution and likelihood evaluation takes six minutes in serial. For 100,000 likelihood evaluations, this would imply over a year of computation time.

true, but unknown, global policy and transition functions. The key advantage is that this object is obtained without solving the model globally. The method therefore mitigates the two principal computational bottlenecks in nonlinear DSGE estimation–global solution and nonlinear filtering–while retaining accuracy.

We benchmark the proposed estimation method using two canonical models. First, in the Diamond (1982)-Mortensen (1982)-Pissarides (1985)-style labor search model, we use a global solution as the data-generating process and show that the method is as accurate as existing nonlinear methods, but at a fraction of the computational cost. Second, we demonstrate our method to the three-equation New Keynesian (NK) model (Gali, 2015) with and without the zero lower bound. The proposed method produces 100,000 posterior draws in under four minutes, which is as fast as it takes to estimate the log-linearized model and several orders of magnitudes (500 to 5000) faster than existing nonlinear approaches.

Main Application We apply the proposed estimation framework to study state dependence in monetary policy transmission within an NK model with labor market frictions. In search models, the flow surplus, i.e., the profitability of job creation, determines how productivity shocks propagate through the economy (Ljungqvist and Sargent, 2017). We show this mechanism extends to monetary policy shocks. In linearized models, the flow surplus is fixed, but in the nonlinear model, it evolves endogenously, giving rise to state-dependent transmission. The method captures this state dependence by solving the model locally along the filtered state path, allowing elasticities to vary. While estimation using global solution methods and nonlinear filters would require several months to generate 100,000 posterior draws,[3] we estimate the model in approximately 25 minutes.

Model-implied state-dependent impulse response functions show that monetary policy shocks affect vacancies and unemployment differently depending on the state of the economy, varying by as much as a factor of two. This generates time variation in the ratio of the cumulative impulse response of inflation relative to unemployment (Phillips Multiplier, Barnichon and Mesters, 2021), which averages -0.07, but can fall to -0.05 in recessions and rises to -0.09 in expansions. These results align closely with evidence from reduced-form state-dependent local pro-

[3] An estimate, based on our computations for the three-equation New Keynesian model, suggests it would take at least 41 weeks of computation time.

jections. More broadly, these results demonstrate that several nonlinear features highlighted in recent empirical work (e.g., Tenreyro and Thwaites, 2016; Benigno and Eggertsson, 2024) can arise endogenously in standard macroeconomic models when solved and estimated nonlinearly – something our method makes computationally feasible.

Extensions We show how the method can be extended to accommodate two widely used exogenous processes: (i) stochastic volatility and (ii) regime switching. The latter includes, for example, models with rare disasters (Barro, 2009). Additionally, the method is extended to heterogeneous agent models. Unlike existing full-information approaches (Winberry, 2018; Liu and Plagborg-Møller, 2023; Auclert et al., 2021), which rely on perturbation and impose certainty equivalence, our approach accommodates aggregate uncertainty in individual decision rules while preserving a linear state-space structure. We illustrate this using a simple heterogeneous household model in which job loss and job finding probabilities are determined by aggregate productivity. The method captures time-varying precautionary saving motives and reveals state dependence and asymmetry in aggregate outcomes that are not well captured by perturbation. The resulting filter is more accurate than the standard Kalman filter applied to the perturbation solution.

Related literature Our methodological contribution is a novel framework for full-information estimation of nonlinear DSGE models. In representative-agent settings, a key benchmark is Fernández-Villaverde and Rubio-Ramírez (2007), who introduce the particle filter to estimate nonlinear DSGE models. While broadly applicable, it is computationally intensive and suffers from the curse of dimensionality. Herbst and Schorfheide (2019) propose the tempered particle filter, which is more stable but at higher computational cost. Farmer (2021) proposes the discretization filter, which is fast, but is limited to small state spaces due to its reliance on tensor products. Winschel and Krätzig (2010) use sparse grids solution methods and parallelization to evaluate the likelihood, but implementation is complex and the computational burden high. All of these methods apply a filter to a separately solved model. In contrast, our approach solves the model dynamically, avoids simulation-based filters, and is both accurate and efficient. Relatedly, Childers et al. (2022) avoid filtering altogether but are limited to low-order perturbation solutions.

In heterogeneous agent models, existing feasible full-information estimation methods rely on perturbation (Auclert et al., 2021; Winberry, 2018; Liu and Plagborg-Møller, 2023), imposing certainty equivalence. Our framework offers a tractable alternative that accommodates nonlinearities in the aggregate dynamics.

In terms of solution method, we build on Den Haan et al. (2015), Levintal (2018), and Mennuni et al. (2024). Levintal (2018) formalizes Taylor Projection, originally used in Krusell et al. (2002), which computes a locally optimal policy rule at a given point in the state space. Fernández-Villaverde and Levintal (2024) apply this approach to a heterogeneous agent model. We apply Taylor Projections (Levintal, 2018) and Dynamic Perturbation (Mennuni et al., 2024) dynamically within our filtering framework, updating the local policy rule at each forecasted state. None of these papers considered full-information estimation, which is the focus of our paper.

Our main application integrates New Keynesian and search-and-matching models, similar to Christiano et al. (2016), Thomas (2011), and Galí et al. (2012). The model is closest to Krause et al. (2008), but a key difference is that they use a linear perturbation solution, which fixes elasticities at steady-state values, whereas our method allows these elasticities to vary over time. This generates state-dependent monetary policy shock transmission, our main contribution relative to this literature. We see the mechanism as complementary to alternative explanations of state dependence based on pricing frictions (Dotsey et al., 1999). Our results also relate to recent work on the Phillips curve slope (Benigno and Eggertsson, 2023; Gitti, 2024), showing that it steepens in tight labor markets. While those papers impose explicit kinks to generate this result, we show it can emerge endogenously from a nonlinear solution.

Outline The rest of this paper is structured as follows. Section 2 presents the method. Section 3 demonstrates the performance of this method using Monte-Carlo simulations from the Diamond-Mortensen-Pissarides model and estimation of the three-equation New-Keynesian model. Section 4 presents the main application. Section 5 presents the quantitative model results and supporting reduced-form evidence. Section 6 discusses extensions with stochastic volatility, regime switching, and heterogeneous households. Section 7 concludes.

2 Local Linear Solutions and the Time-Varying Kalman Filter

This section presents our main methodological contribution: a novel full-information estimation framework for nonlinear DSGE models.

2.1 A General Dynamic Stochastic General Equilibrium model

A standard Dynamic Stochastic General Equilibrium (DSGE) model can be represented as follows (Schmitt-Grohé and Uribe, 2004):

$$\mathbb{E}_t \left[f(y_{t+1}, y_t, x_{t+1}, x_t) \right] = 0, \tag{1}$$

where y_t represents the control variables, and the state variables x_t can be partitioned into endogenous variables $x_{1,t}$ and exogenous variables $x_{2,t}$. We assume the exogenous variables follow a stationary VAR(1):

$$x_{2,t+1} = Ax_{2,t} + B\eta_{t+1}, \tag{2}$$

where η_t is a vector of Gaussian exogenous shocks. Endogenous variables $x_{1,t+1}$ depend on x_t through an unknown nonlinear mapping. Hence, a solution to (1) is characterized by two implicit functions,

$$x_{1,t+1} = h(x_t),$$

which implies the states x_t evolve as

$$x_{t+1} = \begin{pmatrix} h(x_t) \\ Ax_{2,t} \end{pmatrix} + \begin{pmatrix} 0 \\ B \end{pmatrix} \eta_{t+1}, \tag{3}$$

also known as the state transition equation, and the policy function:

$$y_t = g(x_t). \tag{4}$$

A and B are assumed to be known functions of structural parameters (that may have to be estimated), while g and h are the unknown functions to solve for.

2.2 Likelihood Evaluation

Estimating a DSGE model requires specifying an observation equation that maps the observed variables to the model's states and controls:

$$y_t^{\text{obs}} = f(y_t, x_t) + \varepsilon_t^{\text{ME}} = f(g(x_t), x_t) + \varepsilon_t^{\text{ME}} = Z(x_t) + \varepsilon_t^{\text{ME}}, \tag{5}$$

where $\varepsilon_t^{\text{ME}} \overset{i.i.d.}{\sim} N(0, Q)$ is measurement error. To estimate parameters using full-information methods, we must evaluate the model's likelihood function:

$$p(Y_{1:T}^{\text{obs}}) = \prod_{t=1}^{T} p(y_t^{\text{obs}} | Y_{1:t-1}^{\text{obs}}).$$

However, evaluation is complicated by the dependence of y_t^{obs} on the latent state x_t. Computing the sequence $p\left(y_t^{\text{obs}} \mid Y_{1:t-1}^{\text{obs}}\right)$ recursively requires a filter, an algorithm that integrates out the latent state.

Following Herbst and Schorfheide (2016), a general filter can be written as follows. Initialize $p(x_0) = p\left(x_0 | Y_{1:0}^{\text{obs}}\right)$, here, as a Gaussian density with mean $\hat{x}_0$ (e.g., equal to the steady state of the model) and an initial covariance matrix P_0. Next, for $t = 1, \ldots, T$, we iterate between forecasting t given $t-1$, using:

$$p\left(x_t \mid Y_{1:t-1}^{\text{obs}}\right) = \int \underbrace{p\left(x_t \mid x_{t-1}, Y_{1:t-1}^{\text{obs}}\right)}_{\text{state-transition kernel}} p\left(x_{t-1} \mid Y_{1:t-1}^{\text{obs}}\right) dx_{t-1} \quad \text{(Transition Eq.)} \tag{6}$$

$$p\left(y_t^{\text{obs}} \mid Y_{1:t-1}^{\text{obs}}\right) = \int \underbrace{p\left(y_t^{\text{obs}} \mid x_t, Y_{1:t-1}^{\text{obs}}\right)}_{\text{observation kernel}} p\left(x_t \mid Y_{1:t-1}^{\text{obs}}\right) dx_t \quad \text{(Observation Eq.)} \tag{7}$$

and updating with Bayes rule:

$$p\left(x_t \mid Y_{1:t}^{\text{obs}}\right) = p\left(x_t \mid y_t^{\text{obs}}, Y_{1:t-1}^{\text{obs}}\right) = \frac{p\left(y_t^{\text{obs}} \mid x_t, Y_{1:t-1}^{\text{obs}}\right) p\left(x_t \mid Y_{1:t-1}^{\text{obs}}\right)}{p\left(y_t^{\text{obs}} \mid Y_{1:t-1}^{\text{obs}}\right)}. \tag{8}$$

Traditionally, the problem of solving the model, that is, obtaining functional forms for the state-transition equation (3) and the policy function (4), is treated separately from the filtering problem in Equations (6)–(8). However, the choice of solution

method, and in particular the functional forms of g and h, directly affects the complexity of the filtering problem.

When the functions $x_{1,t+1} = h(x_t)$ and $y_t = g(x_t)$ in Equations (3)–(4), together with the observation equation (5), are assumed to be linear, the state-transition and observation kernels are Gaussian. In this case, Equations (6)–(7) reduce to convolutions of normal densities, and the filtering problem simplifies to the Kalman filter. This corresponds to the standard approach in which a DSGE model is solved using a first-order perturbation and filtered via the Kalman filter (for a textbook treatment, see Herbst and Schorfheide, 2016). While easy to implement and computationally efficient, first-order perturbations have important limitations: they impose certainty equivalence, assume constant elasticities to shocks, and may yield poor approximations far from the steady state (Judd et al., 2017).

Higher-order perturbations (Judd, 1998) address some shortcomings of linear solutions but introduce additional complexity, require pruning for stability (Andreasen et al., 2018), and remain centered around a single expansion point. Global solution methods, such as those based on projection techniques, provide accuracy across the entire state space but are computationally intensive. In either case, when the state-transition function (3) and/or the policy function (4) are nonlinear, likelihood evaluation requires nonlinear filters, which can be costly for larger models.

An important insight is that although general nonlinear solutions complicate filtering, the Kalman filter remains valid when the state-transition and observation equations take the form (Hamilton, 1994; Durbin and Koopman, 2012):

$$x_{t+1} = c\left(Y_{1:t-1}^{\text{obs}}\right) + T\left(Y_{1:t-1}^{\text{obs}}\right) x_t + R\eta_{t+1}, \tag{9}$$

$$y_t = d\left(Y_{1:t-1}^{\text{obs}}\right) + Z\left(Y_{1:t-1}^{\text{obs}}\right) x_t + \varepsilon_t^{\text{ME}}, \tag{10}$$

where $c(\cdot)$, $T(\cdot)$, $d(\cdot)$, and $Z(\cdot)$ are arbitrary functions of the observed data history $Y_{1:t-1}^{\text{obs}}$. Conditional on data up to $t-1$, the state-transition and observation equations are linear and Gaussian. As a result, Equations (6)–(8) reduce to convolutions of normal densities, and the Kalman filter remains optimal.

Now suppose that, given the data history $Y_{1:t-1}^{\text{obs}}$, a state forecast $\hat{x}_{t|t-1}$ is obtained, and we approximate the functions g and h using a *local linear* specification, centered

at x and parameterized by $\Theta = (\Theta_1, \Theta_2, \Theta_3, \Theta_4)$:

$$\tilde{g}(x_t; \Theta) = \Theta_1(x) + \Theta_2(x)x_t, \tag{11}$$

$$\tilde{h}(x_t; \Theta) = \Theta_3(x) + \Theta_4(x)x_t. \tag{12}$$

Note that Θ is an implicit function of the point of approximation x. Local linear model solutions of the form in Equations (11)-(12) arise in Den Haan et al. (2015), Levintal (2018), and Mennuni et al. (2024), we elaborate on this in the next subsection. Assume that we approximate the solution at $x = \hat{x}_{t|t-1}$. Under these assumptions, the state-space system becomes:

$$y_t^{\text{obs}} = d_t + Z_t x_t + \varepsilon_t^{\text{ME}}, \tag{13}$$

$$x_{t+1} = \underbrace{\begin{pmatrix} \Theta_3\left(\hat{x}_{t|t-1}\right) \\ 0 \end{pmatrix}}_{c_t} + \underbrace{\begin{pmatrix} \Theta_4\left(\hat{x}_{t|t-1}\right) \\ A \end{pmatrix}}_{T_t} x_t + \underbrace{\begin{pmatrix} 0 \\ B \end{pmatrix}}_{R} \eta_{t+1}, \tag{14}$$

where $c_t \equiv c(\hat{x}_{t|t-1})$ and $T_t \equiv T(\hat{x}_{t|t-1})$. The coefficients $d_t \equiv d(\hat{x}_{t|t-1})$ and $Z_t \equiv Z(\hat{x}_{t|t-1})$ may include elements of $\Theta(\hat{x}_{t|t-1})$ as well as other model parameters, depending on the observables. Since $\hat{x}_{t|t-1}$ is a function of $Y_{1:t-1}^{\text{obs}}$, Equations (13)–(14) are consistent with the form in Equations (9)–(10) and the Kalman filter.

While the solution in Equations (11)–(12) and the resulting state-space model are locally linear, the structure offers greater flexibility than standard linear perturbation methods by allowing model dynamics to vary with the current state forecast. This enables the system to capture nonlinearities and state-dependent behavior, as discussed in the next subsection.

2.3 Local Linear Solutions

Next, we detail how to obtain solutions of the form in Equations (11)-(12). For our implementation, we adopt a dynamic version of the Taylor projection method (Levintal, 2018) because of its computationally efficiency. However, the filtering framework in this paper is flexible and is also compatible with alternative local linear solution methods.

First, assume the policy function $g(x_t)$ and law of motion $h(x_t)$ take the form:

$$g(x_t) = \Theta_1 + \Theta_2 x_t, \quad h(x_t) = \Theta_3 + \Theta_4 x_t.$$

This implies the following for current and future controls and future states:

$$\tilde{y}_t = \Theta_1 + \Theta_2 x_t \tag{15}$$

$$\tilde{x}_{t+1} = \begin{pmatrix} \Theta_3 \\ 0 \end{pmatrix} + \begin{pmatrix} \Theta_4 \\ A \end{pmatrix} x_t + \begin{pmatrix} 0 \\ B \end{pmatrix} \eta_{t+1} \tag{16}$$

$$\tilde{y}_{t+1} = \Theta_1 + \Theta_2 \tilde{x}_{t+1} \tag{17}$$

The approximate residual function $R(x_t, \Theta)$ is constructed by substituting (15)-(17) into the equilibrium condition (1):

$$R(x_t, \Theta) = \mathbb{E}_t \left[f(\tilde{y}_{t+1}, \tilde{y}_t, \tilde{x}_{t+1}, x_t) \right]. \tag{18}$$

The coefficients Θ are chosen such that the residual (18) is approximately zero around x, by equating the first-order Taylor expansion of the residual function at x to zero, which implies:

$$R(x, \Theta^*) = 0, \quad \nabla_x R(x_t, \Theta^*)\big|_{x_t = x} = 0.$$

Solving this system at a given state x yields a set of state-dependent coefficients $\Theta(x)$, which define the approximate solutions $\tilde{g}(x_t, \Theta(x))$ and $\tilde{h}(x_t, \Theta(x))$. As noted above, we set $x = \hat{x}_{t|t-1}$ to construct a sequence of solutions at the forecasted states of the filter. These approximations are locally accurate around each x, and, because the solution is updated dynamically at $x = \hat{x}_{t|t-1}$ for $t = 1, \ldots, T$, they remain accurate throughout the sample.

Dynamic Perturbation. An alternative way to obtain local linear solutions of the form in Equations (11)–(12) is the Dynamic Perturbation (DP) method of Mennuni et al. (2024). Like Taylor Projection, DP approximates the policy function and law of motion locally by linear functions. The key difference is that DP does not determine the coefficients Θ by imposing that a single residual function is locally zero and

locally flat at a point x. Instead, DP constructs a sequence of local approximations along an equilibrium path.

To see this in our notation, suppose that at date $t+1$ we have a local linear approximation characterized by $\Theta(\hat{x}_{t+1|t})$. Given a current state $x_t = x$, DP first solves the equilibrium conditions for the current controls y_t and next-period endogenous states $x_{1,t+1}$, taking the next-period local policy rule as given. It then applies the Implicit Function Theorem to compute the derivatives of y_t and $x_{1,t+1}$ with respect to x_t. These levels and derivatives define the coefficients $\Theta(x)$ in Equations (11)–(12). Repeating this argument along the path yields a time-varying sequence of local linear decision rules.

Relative to Taylor Projection, DP has two attractive features for our purposes. First, it allows the local approximation used at date t to differ from the approximation used at date $t+1$, which improves accuracy when the equilibrium path moves away from the steady state. Second, DP extends naturally to environments with regime changes or occasionally binding constraints. This is especially useful in our applications, since it allows the solution to accommodate the zero lower bound and the associated shift in local dynamics. The potential cost is computational. Taylor Projection requires a local approximation at only one state, whereas DP constructs local approximations sequentially along the equilibrium path. We explore these trade-offs in the applications.

Properties of the solution Any differentiable function can be locally approximated by a linear function, with coefficients that depend on the point of approximation. By evaluating these approximations at multiple points in the state space, the solution captures global nonlinear dynamics. For example, allowing the coefficients Θ to vary with the state enables the model to capture features such as state-dependent elasticities to shocks.

A second important property of the solution approach is that, unlike standard first-order perturbation methods, Taylor projections and Dynamic Perturbation do not impose certainty equivalence. Because the residual function $R(x_t, \Theta)$ includes expectations over future shocks, the resulting decision rule coefficients depend on the stochastic properties of the exogenous states, such as shock volatility.

One potential computational bottleneck is that the residual function involves expectations, which would ordinarily require numerical integration. However, when policies are linear in logs and shocks are Gaussian, these expectations can often be computed analytically, including in several of our applications.[4] This yields an exact nonlinear system, which improves both speed and accuracy: it eliminates integration error, accelerates residual evaluation, and provides exact Jacobians for use with nonlinear solvers.

2.4 Time-Varying Kalman Filter

Taking stock, the time-varying linear state-space system in Equations (13)–(14), together with the local linear solution method outlined in the previous subsection, give rise to the filtering procedure described in Algorithm 1. In words, Algorithm 1 computes a local linear approximation of the policy function g and the law of motion h at the forecasted state $\hat{x}_{t|t-1}$, which represents the best estimate of the current state x_t based on data through period $t-1$. This approximation is then mapped into the linear state-space form given by Equations (13) and (14), and the Kalman filter is used to generate a forecast for the next state, $\hat{x}_{t+1|t}$. The procedure is then repeated: a new local linear solution is computed at $\hat{x}_{t+1|t}$, mapped into state-space form, and used to forecast $\hat{x}_{t+2|t+1}$, and so on.

This filtering approach differs fundamentally from traditional methods, which solve the model once per likelihood evaluation and then apply a filter. In contrast, the solution here is constructed dynamically within the filtering procedure at each forecasted state, providing a computationally efficient means of accurately approximating global model dynamics. Because they are computed only at the relevant states implied by the data, they eliminate the need for costly global solution and nonlinear filtering procedures.

The corresponding smoothing procedure is presented in Algorithm 2 in Appendix A. The Kalman smoother relies on the same sequence of system matrices computed in Algorithm 1 and therefore does not require re-solving the model.

[4] When relevant, we provide additional details on this step in the Appendix. For a normally distributed random variable, $\mathbb{E}[e^{cx}] = e^{c\mu+\frac{1}{2}c^2\sigma^2}$.

Algorithm 1 Time-Varying Kalman Filter

Initialize: Set $t = 0$, start x_0 in the steady state, and initialize covariance $P_{0|0}$.
while $t \leq T$ **do**

Solution Step: Solve the model using Taylor Projections at $\hat{x}_{t|t-1}$, obtaining the state space system in Equations (13)-(14).

Update Step:

Compute the Kalman gain:

$$F_t = Z_t P_{t|t-1} Z_t' + H \tag{19}$$

$$K_t = T_t P_{t|t} Z_t' F_t^{-1} \tag{20}$$

Update the state estimate using the new observation y_t:

$$v_t = y_t^{\text{obs}} - Z_t \hat{x}_{t|t-1} - d_t \tag{21}$$

$$\hat{x}_{t|t} = \hat{x}_{t|t-1} + K_t v_t \tag{22}$$

Update the covariance:

$$P_{t|t} = (I - K_t Z_t) P_{t|t-1} \tag{23}$$

Prediction step:

Compute the predicted state estimate:

$$\hat{x}_{t+1|t} = T_t \hat{x}_{t|t} + c_t \tag{24}$$

Compute the predicted covariance:

$$P_{t+1|t} = T_t P_{t|t} T_t' + R Q R' \tag{25}$$

Advance time: Set $t \leftarrow t + 1$ and repeat.
end while

2.5 Relation to the Extended Kalman Filter

The extended Kalman filter (EKF) provides the natural oracle benchmark for our approach. Suppose the true equilibrium policy $g^*(x_t)$ and endogenous transition $h^*(x_t)$ are known. Then the nonlinear state-space system can be written as

$$y_t^{\text{obs}} = Z(x_t) + \varepsilon_t^{\text{ME}}, \tag{26}$$

$$x_{t+1} = \begin{pmatrix} h^*(x_t) \\ A x_{2,t} \end{pmatrix} + \begin{pmatrix} 0 \\ B \end{pmatrix} \eta_{t+1}, \tag{27}$$

where $Z(x_t) = f(g^*(x_t), x_t)$ in the notation of (5). The EKF then constructs a time-varying linear state-space system by taking a first-order Taylor expansion of g^* and h^* around the forecasted state x:

$$g^*(x_t) \approx g^*(x) + D_x g^*(x)(x_t - x), \tag{28}$$

$$h^*(x_t) \approx h^*(x) + D_x h^*(x)(x_t - x). \tag{29}$$

Thus, if the true global solution were available, the EKF representation would be immediate. The relevance of this oracle benchmark for our framework is that the same first-order objects of (28)-(29) can be recovered from the equilibrium system itself, if the true continuation policy g were known. Fix a current state $x_t = (x'_{1,t}, x'_{2,t})'$, and let g denote a candidate continuation policy for future controls. Conditional on g, the period-t equilibrium system (1) implicitly defines an implied current control vector and an implied endogenous transition,

$$\hat{g}(x_t; g), \qquad \hat{h}(x_t; g),$$

with next-period state

$$x_{t+1} = \begin{pmatrix} \hat{h}(x_t; g) \\ A x_{2,t} \end{pmatrix} + \begin{pmatrix} 0 \\ B \end{pmatrix} \eta_{t+1}. \tag{30}$$

Equivalently, $(\hat{g}, \hat{h})$ is defined by the period-t equilibrium system

$$\mathbb{E}_t \left[f\left(g(x_{t+1}), \hat{g}(x_t; g), x_{t+1}, x_t\right) \right] = 0, \qquad x_{t+1} \text{ given by (30).} \tag{31}$$

Hence any continuation policy g induces a one-step operator

$$g \mapsto \left(\hat{g}(\cdot; g), \hat{h}(\cdot; g)\right).$$

Now let (g^*, h^*) denote the true equilibrium policy and endogenous transition. If the continuation policy used in (31) is the true policy g^*, then the induced objects coincide with the truth:

$$\hat{g}(x_t; g^*) = g^*(x_t), \qquad \hat{h}(x_t; g^*) = h^*(x_t). \tag{32}$$

That is, the true equilibrium pair is a fixed point of the operator induced by the period-t equilibrium system.

Under standard local regularity conditions, this fixed-point property extends to first derivatives. Specifically, if the equilibrium system is continuously differentiable and the Jacobian with respect to the current unknowns $(y_t, x_{1,t+1})$ is nonsingular, then the implicit function theorem implies

$$D_x \hat{g}(x; g^*) = D_x g^*(x), \qquad D_x \hat{h}(x; g^*) = D_x h^*(x). \tag{33}$$

Accordingly, if the true continuation policy were known, the equilibrium system would recover both the level and the Jacobian of the true policy and transition functions at the expansion point.

Consider now a first-order local equilibrium solution at a point x, written as

$$\tilde{g}(x_t; x) = a_g(x) + b_g(x)(x_t - x), \tag{34}$$

$$\tilde{h}(x_t; x) = a_h(x) + b_h(x)(x_t - x). \tag{35}$$

By (32)–(33), if the continuation policy used to construct the local solution is g^*, then

$$a_g(x) = g^*(x), \qquad b_g(x) = D_x g^*(x), \qquad a_h(x) = h^*(x), \qquad b_h(x) = D_x h^*(x). \tag{36}$$

Thus, in the oracle case, the local equilibrium solution coincides with the first-order Taylor expansion of the true global solution. Comparison of (36) with (28)–(29) therefore shows that the EKF is the oracle case of our framework.

The oracle case is, by construction, infeasible. If g^* were known, no solution method would be required. The role of a first-order local solution method is therefore to approximate the continuation policy entering (31). This interpretation applies to both first-order Taylor projection and first-order dynamic perturbation. Taylor projection closes the local system by restricting future policy to the same local rule used at the current point. Dynamic perturbation instead closes the system by constructing the continuation policy along an auxiliary path. In both cases, the quality of the resulting local solution is determined by the quality of the induced approximation to g^*.

This dependence can be stated locally in terms of the operator $g \mapsto (\hat{g}(\cdot; g), \hat{h}(\cdot; g))$. If the equilibrium system is continuously differentiable and its Jacobian with respect to the current unknowns is nonsingular at (x, g^*), then there exist a neighborhood $\mathcal{N}(x)$ of x and a constant $K_0(x) > 0$ such that

$$\|\hat{g}(x; g) - g^*(x)\| + \|\hat{h}(x; g) - h^*(x)\| \leq K_0(x) \sup_{z \in \mathcal{N}(x)} \|g(z) - g^*(z)\|, \tag{37}$$

for all continuation policies g sufficiently close to g^*. If, in addition, the equilibrium system is twice continuously differentiable in the current unknowns and the state, then there exists $K_1(x) > 0$ such that

$$\begin{aligned} &\|D_x\hat{g}(x; g) - D_x g^*(x)\| + \|D_x\hat{h}(x; g) - D_x h^*(x)\| \\ &\qquad \leq K_1(x) \left(\sup_{z \in \mathcal{N}(x)} \|g(z) - g^*(z)\| + \sup_{z \in \mathcal{N}(x)} \|D_z g(z) - D_z g^*(z)\| \right). \end{aligned} \tag{38}$$

Thus both level and derivative errors are locally controlled by the continuation-policy error. This yields the relevant comparison with the EKF. The oracle EKF presupposes the true global solution and then linearizes it. Our approach instead solves the equilibrium system locally after closing it with an approximation to the unknown continuation policy. The oracle case obtains when the continuation policy used to close the local system coincides with g^*, in which case the induced linear state-space system is exactly the EKF representation. More generally, when the continuation-policy approximation delivered by these methods is accurate, the resulting local linear system is correspondingly close to the oracle EKF.

Our main contribution is that we obtain this object without needing to know or compute the global nonlinear solution: we approximate the unknown continuation policy, solve the equilibrium system locally, and then apply the time-varying Kalman filter. In this sense, the method delivers a computationally tractable approximation to the oracle EKF.

3 Two Canonical Examples

In this section, we compare the performance of our proposed estimation framework to existing methods using simulations of the Diamond-Mortensen-Pissarides

model, and further demonstrate the method by revisiting the textbook three-equation New Keynesian model, with and without the zero-lower bound. Both models are known to be poorly approximated by standard perturbation approaches (Petrosky-Nadeau and Zhang, 2017; Judd et al., 2017).

3.1 Diamond-Mortensen-Pissarides model

We briefly describe the model environment, which is standard. The only non-standard assumption is the one made with respect to the timing of separations and hires. Following the literature on labor search in NK models (Christiano et al., 2016), we assume workers who lose their jobs at the beginning of the period can search within the period for a new job.[5]

Firms post vacancies V_t to maximize the present discounted value of profit taking wages as given:

$$\mathbb{E}_0 \left[\sum_{t=1}^{\infty} \beta^t \left\{ \left(e^{z_t} - W_t\right) N_t - \kappa V_t \right\} \right] \quad \text{subject to} \quad N_t = (1-\delta) N_{t-1} + q_t V_t,$$

where the flow payoff is output $e^{z_t} N_t$, net of wage expenditures $W_t N_t$ and vacancy posting costs κV_t, δ is the job destruction rate, and q_t the vacancy filling rate. In equilibrium, the Nash wage is given by $W_t = \eta e^{z_t} + (1-\eta)\nu$, where η is the worker's bargaining weight, and ν is the outside option of the worker. The model consists of one policy: θ_t, the natural log of market tightness, and one state, z_t, the marginal product of labor. Hence, the equilibrium is characterized by two equations:

$$\begin{aligned} \frac{c}{q_t} &= (1-\eta)\left(e^{z_t} - \nu\right) + \beta(1-\delta)\mathbb{E}_t \left[\frac{c}{q_{t+1}} \right] \\ z_{t+1} &= \rho z_t + \varepsilon_{t+1}, \quad \varepsilon_{t+1} \sim N\left(0, \sigma^2\right) \end{aligned}$$

We assume the matching function is Cobb-Douglas[6] which implies

$$q_t = \chi e^{-\alpha \theta_t}$$

[5] This assumption is typically justified as a way of making low-frequency (quarterly) NK models conform with labor markets where most unemployment spells last only a few weeks. According to the estimate of Ahn and Hamilton (2022), two-thirds of workers exit unemployment within the first quarter of an unemployment spell.

[6] Note, scaling the matching function by some matching efficiency is identical to rescaling the vacancy cost c.

where α is an elasticity, and χ matching efficiency. Let

$$\hat{\theta}_t = \theta_t - \theta_{ss},$$

denote the log deviation of θ_t from its steady state value θ_{ss}. Using this definition and the functional form of the matching function allows us to rewrite the equilibrium job-creation condition as:

$$e^{\alpha\hat{\theta}_t} = \left(1 - \beta(1-\delta)\right)\frac{e^{z_t} - \nu}{1-\nu} + \beta(1-\delta)\mathbb{E}_t\left[e^{\alpha\hat{\theta}_{t+1}}\right] \tag{39}$$

Model Solution: Log-linearization and higher-order perturbations The log-linear solution as well as higher-order perturbations for this model can be computed analytically. Define $\kappa := \beta(1-\delta)$. The log-linear policy rule for $\hat{\theta}_t = \Gamma_{ss} z_t$ has

$$\Gamma_{ss} = \frac{1-\kappa}{\alpha(1-\nu)(1-\kappa\rho)}$$

with a constant elasticity of market tightness to marginal product of labor $\epsilon(\theta_t, z_t) = \Gamma_{ss}$. Derivations are detailed in the Appendix.

Model Solution: Taylor Projection The DMP model above has one state (productivity, z_t) and one policy to solve for: market tightness $\hat{\theta}_t = g(z_t)$. Hence, mapping this back to our previous notation, our state $x_t \equiv z_t$ and our control $y_t \equiv \hat{\theta}_t$. We approximate the policy function by:

$$\hat{\theta}_t = \Gamma_1 + \Gamma_2(z_t - z_0) \tag{40}$$

where local policy coeffients (Γ_1, Γ_2) implicitly depend on the approximation point z_0 and model parameters. Because the exogenous state is a Gaussian AR(1), we can rewrite

$$\hat{\theta}_{t+1}(z, \varepsilon) = \Gamma_1 + \Gamma_2(\rho z + \sigma\varepsilon' - z_0)$$

The TP method identifies $(\Gamma_1,\ \Gamma_2)$ by imposing that the equilibrium residual $R(z)$ of the job-creation condition is locally zero and locally flat:

$$R(z_t) = 0, \qquad \frac{\partial R(z)}{\partial z}\Big|_{z=z_t} = 0.$$

The residual function simplifies to:

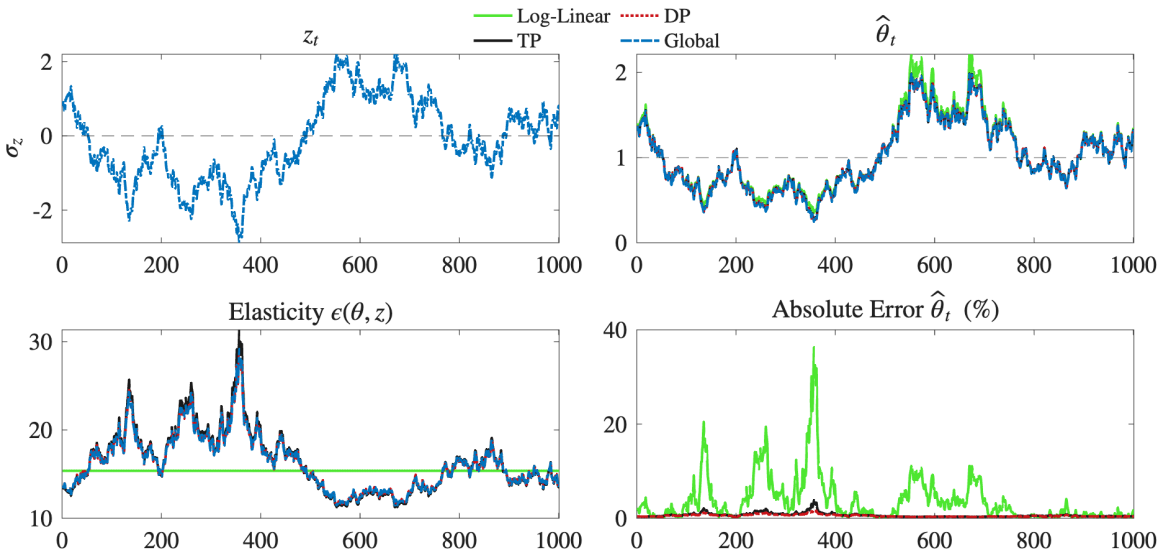
$$\begin{aligned} R(z) &= e^{\alpha\hat{\theta}_t(z)} - (1-\kappa)\,\frac{e^z-\nu}{1-\nu} - \kappa\,\mathbb{E}_t\left[e^{\alpha\hat{\theta}_{t+1}(z,\varepsilon)}\right] \\ &= e^{\alpha(\Gamma_1+\Gamma_2(z-z_0))} - (1-\kappa)\,\frac{e^z-\nu}{1-\nu} - \kappa\,\mathbb{E}_{z'}\left[e^{\alpha(\Gamma_1+\Gamma_2(\rho z+\sigma\varepsilon'-z_0))}\Big|z\right] \end{aligned}$$

Model Solution: Dynamic Perturbation The Dynamic Perturbation approach of Mennuni et al. (2024) is also based on a local linear approximation of the policy rule, but differs from Taylor Projection in how the coefficients are obtained. Rather than choosing (Γ_1, Γ_2) so that the residual of the job-creation condition is locally zero and locally flat at z_0, Dynamic Perturbation computes the policy coefficients recursively along the equilibrium path. Given an approximation for next period's policy rule, the method solves the current equilibrium condition for $\hat{\theta}_t$ and then uses implicit differentiation to obtain the slope of the policy rule with respect to the current state z_t. This yields a sequence of time-varying local coefficients $(\Gamma_{1,t}, \Gamma_{2,t})$, indexed by the point of approximation, rather than a single approximation tied to one state. In the Appendix, we show that for the DMP model this recursion admits an analytical characterization, so the Dynamic Perturbation solution can be implemented without numerically solving a nonlinear system at each step.

Model Solution: Global For the global model solution, we solve the model using time iteration on the job creation condition, using a finely discretized grid of z_t. We use Chevychev interpolation to evaluate the policy in between grid points. Since the model only has one state and one policy, the global model solution is computationally inexpensive.

Comparing Model Solutions Figure 1 compares four solution methods: (i) a global solution that approximates the policy function by projecting onto a polynomial basis, (ii) a dynamic Taylor projection recomputed at each point along the simulated path, (iii) a dynamic perturbation solution recomputed at each point

Figure 1: Comparison of log-linear, global, dynamic Taylor projection, and dynamic perturbation solutions of the DMP model for the same path of productivity z_t of length $T = 1000$.



along the simulated path, and (iv) a log-linear solution around the non-stochastic steady state. All methods are evaluated on the same productivity realization (top-left panel), yet they generate materially different dynamics for market tightness. The global solution, dynamic Taylor projection, and dynamic perturbation solutions track each other closely throughout the simulation, whereas the log-linear approximation exhibits sizable discrepancies, with deviations of up to 35% in market tightness. Moreover, the dynamic Taylor projection and dynamic perturbation solutions replicate the time-varying elasticity of market tightness with respect to productivity, a key nonlinearity of the DMP model; in contrast, log-linearization imposes a constant elasticity.

State-Space Representation To make explicit how the Taylor projection or Dynamic Perturbation solution maps into a linear state space model, assume we observe market tightness and log wages, with measurement errors. The local linear solution methods imply a linear mapping of log market tightness $\hat{\theta}_t$ to the state, and wages $w_t = \log W_t / W_{ss}$ can be linearized using a first order expansion around the current state forecast $\hat{z}_{t|t-1}$ as:

$$w(z_t) \approx w\left(\hat{z}_{t|t-1}\right) + \frac{\partial w(z)}{\partial z}\Big|_{z=\hat{z}_{t|t-1}} (z_t - \hat{z}_{t|t-1}).$$

This implies the following state-space representation:

$$\begin{pmatrix} \theta_t^{\text{obs}} \\ w_t^{\text{obs}} \end{pmatrix} = \begin{pmatrix} \Gamma_1\left(\hat{z}_{t|t-1}\right) - \Gamma_2\left(\hat{z}_{t|t-1}\right)\hat{z}_{t|t-1} \\ \log\left(\frac{\eta e^{\hat{z}_{t|t-1}} + (1-\eta)\nu}{\eta + (1-\eta)\nu}\right) - \frac{\hat{z}_{t|t-1}\eta e^{\hat{z}_{t|t-1}}}{\eta e^{\hat{z}_{t|t-1}} + (1-\eta)\nu} \end{pmatrix} + \begin{bmatrix} \Gamma_2\left(\hat{z}_{t|t-1}\right) \\ \frac{\eta e^{\hat{z}_{t|t-1}}}{\eta e^{\hat{z}_{t|t-1}} + (1-\eta)\nu} \end{bmatrix} z_t + \varepsilon_t^{ME}$$

$$z_{t+1} = \rho_z z_t + \eta_{t+1}, \quad \eta_t \sim (0, \sigma_z^2).$$

We can then use Algorithm 1 to filter the underlying states and evaluate the likelihood of this model.

Filter Accuracy: Euler Errors To evaluate the accuracy of the solution method, we compute Euler errors, which measure the extent to which the policy rule approximates the decision implied by the model's equilibrium condition, in this case the job creation condition (39). As per our theoretical framework, the filter accuracy is determined by how well a policy rule computed at a local point $\hat{z}_{t|t-1}$ approximates behavior at the future states, z_{t+1}. To asses this, at each period t, we use the policy rule computed at $\hat{z}_{t|t-1}$ to evaluate the expected Euler error implied by the equilibrium condition at future states $z_{t+1} \sim N(\hat{z}_{t+1|t}, P_{t+1|t})$. Based on a simulation of $T = 10{,}000$ periods from a globally solved model with parameters reported in Table 2, we find that the average (over time) expected Euler error is -4.46 for Taylor Projection, and -4.27 for Dynamic Perturbation, with 99% of realized errors below -3.59 and -3.33 respectively. This indicates that the policy rule remains highly accurate even when applied one step ahead, before recomputing the solution at the next forecast.

Table 1: Simulated Euler Errors for log-linear solution and the local linear policy rules of Taylor Projection and Dynamic Perturbation. For the local linear methods, the policy is computed at $\hat{z}_{t|t-1}$ and the Euler error is evaluated at future states $z_{t+1} \sim N(\hat{z}_{t+1|t}, P_{t+1|t})$ for a simulation of length $T = 10,000$.

	Log-Linear	Taylor Projection	Dynamic Perturbation
Mean	−1.74	−4.46	−4.27
90th percentile	−1.28	−4.06	−3.83
99th percentile	−1.06	−3.59	−3.33

Note: Calibration: $r = 0.04$, $\beta = \left(\frac{1}{1+r}\right)^{1/52}$, $\alpha = 0.50$, $\eta = 0.50$, $\nu = 0.85$; $\theta_{ss} = 1$, $q_{ss} = 0.5$, $u_{ss} = 0.1$; $\rho = 0.9895$, $\sigma = 0.0034$.

Monte Carlo Next, we evaluate the performance of the various filters in a simulation.

Table 2: Comparison of solution and filtering methods for the DMP model at $T = 200$. MSE is scaled by the unconditional variance of the corresponding variable.

Method	Particles	$100 \times \text{MSE}_\theta$	$100 \times \text{MSE}_w$	$100 \times \text{MSE}_z$	Time (s)
Global + EKF	–	1.53	1.53	0.67	0.081
DP + TV-KF	–	1.54	1.54	0.67	0.036
TP + TV-KF	–	1.55	1.54	0.67	0.071
Log-linear + KF	–	2.42	2.21	0.89	0.002
2nd-order pert. + PF	200	1.64	1.63	0.75	0.021
	2,000	1.53	1.53	0.67	0.086
	20,000	1.52	1.52	0.67	0.269
3rd-order pert. + PF	200	1.61	1.62	0.76	0.023
	2,000	1.51	1.51	0.68	0.096
	20,000	1.50	1.50	0.67	0.311
6th-order pert. + PF	200	1.61	1.62	0.76	0.035
	2,000	1.51	1.51	0.68	0.165
	20,000	1.50	1.50	0.67	0.501
Global + PF	200	1.61	1.61	0.76	0.111
	2,000	1.51	1.51	0.68	0.278
	20,000	1.50	1.50	0.67	1.558

Note: Calibration: $r = 0.04$, $\beta = \left(\frac{1}{1+r}\right)^{1/52}$, $\alpha = 0.50$, $\eta = 0.50$, $\nu = 0.85$; $\theta_{ss} = 1$, $q_{ss} = 0.5$, $u_{ss} = 0.1$; $\rho = 0.9895$, $\sigma = 0.0034$.

We simulate 1,000 datasets from the DMP model using a global solution method, for $T = 200$ which is comparable to the length of a typical macro dataset. We add measurement error of 20% of the true standard deviation to construct observable market tightness and compare five solution–filtering methods: (i) linear perturbation with Kalman Filter (Linear+KF), (ii-iv) second, third and sixth order perturbations with Particle Filter, (v) global solution with Particle Filter (Global+PF), (vi) Taylor Projection with Time-Varying Kalman Filter (TP+TV-KF), (vii) Dynamic Perturbation with Time-Varying Kalman Filter (DP+TV-KF), and and (viii) global solution with Extended Kalman Filter (Global+EKF). We fix the structural model parameters to their true values (see note in Table 2), and our goal is to assess how well each method recovers the unobserved states from the simulated data. Table 2 evaluates

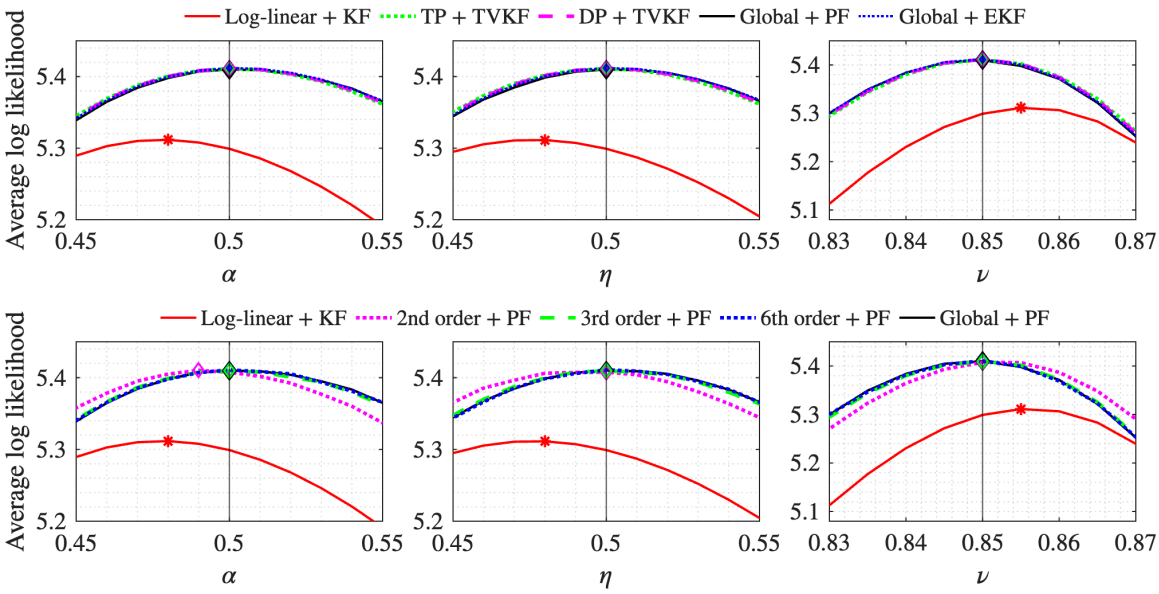
performance by comparing the mean squared error (MSE) of the true and filtered state. Additionally, the table reports computation times for each approach.

As per Table 2, log-linear+KF is the fastest method (0.001 seconds for a single likelihood-evaluation), but it has substantially higher error: the MSE is 2.42 for tightness, 2.21 for wages, and 0.89 for TFP, compared to roughly 1.50–1.55, 1.50–1.54, and 0.67 for the nonlinear and locally time-varying methods as well as the higher-order perturbations. As one would expect, a particle filter with enough particles achieves the lowest MSEs, but computation time rises sharply with the number of particles: from 0.1 seconds (200 particles) to 1.6 seconds (20,000 particles). Moreover, with only 200 particles, the particle filter is less accurate than the local linear alternatives: for example, Global+PF with 200 particles delivers an MSE for TFP of 0.76 versus 0.67 for DP+TV-KF and TP+TV-KF. Consistent with our theory, DP+TV-KF, TP+TV-KF, and Global+EKF have very similar MSEs at low computational cost. Note that in this small model, the global solution is fast, so Global+EKF and Global+PF are not prohibitively expensive; however, in larger and more computationally demanding models, the local time-varying approaches are more scalable. A third and sixth order perturbation with enough particles is comparably accurate to the global model, but computationally more intensive than DP+TV-KF and TP+TV-KF.

Comparing Likelihoods Next, we compare likelihood functions. Data are simulated from the global solution with measurement error in market tightness (20% of standard deviation) and wages (20%). We simulate a data set of length $T = 5,000$. Figure 2 shows two times three panels of likelihood functions where all parameters are kept fixed at their true value, expect for one parameter that is varied on a grid. We consider matching elasticity α, outside option ν and bargaining power η.

The figure shows that the Log-linear+KF likelihoods lead to inconsistent estimates. In contrast, TP+TV-KF, Global+PF (2,000 particles), and Global+EKF yield almost indistinguishable likelihoods around the true parameter values, with maximizers coinciding with the truth. The second row in Figure 2 shows the perturbation approaches alongside the global solution, confirming the results of Table 2 that a third order perturbation is approximately as accurate as the global solution for this particular model. Second-order perturbations still lead to biased estimates, albeit with smaller bias than the log-linearization.

Figure 2: Comparing likelihoods for match elasticity α, outside option ν and bargaining power η.



Note: Calibration: $r = 0.04$, $\beta = \left(\frac{1}{1+r}\right)^{1/52}$, $\alpha = 0.50$, $\eta = 0.50$, $\nu = 0.85$; $\theta_{ss} = 1$, $q_{ss} = 0.5$, $u_{ss} = 0.1$; $\rho = 0.9895$, $\sigma = 0.0034$. *Figure compares likelihoods computed based on the time-varying Kalman filter with Dynamic Perturbation and Taylor Projection, the Particle Filter + global model solution, Extended Kalman filter with global model solution, and the linearized model with Kalman filter (red solid line). Note that all lines except the log-linear-based likelihood are on top of each other. Dots represent the maximum likelihood estimate. Based on a simulation of length* $T = 5000$ *from the global model solution. All other parameters are kept constant at their true values.*

3.2 Estimating the Three-Equation New Keynesian Model with and without Zero Lower Bound

Our next example is the canonical three-equation New Keynesian model in Gali (2015), with and without a zero lower bound on the interest rate. Given the model is very well known, we leave most model details to Appendix C. A minimal state-space representation of the model consists of the state variables: productivity a_t, discount factor shocks d_t and monetary policy shocks m_t, all following an AR(1), collected in $x_t = (a_t, d_t, m_t)$, and policy functions for inflation and employment $\{\Pi(x_t), N(x_t)\}$. These policies are determined by two equilibrium conditions: the Euler equation (IS curve) and the optimal price-setting condition (New Keynesian Phillips Curve). An auxiliary Taylor Rule determines the nominal interest rate R_t.

Given the minimal state representation, we solve for two policies $\pi_t = \log(\Pi_t/\Pi)$ and $n_t = \log(N_t/N)$, that is inflation and employment in log deviations from their

steady state values:

$$g^{\pi}(a_t, d_t, m_t) = \alpha_0 + \alpha_1 a_t + \alpha_2 d_t + \alpha_3 m_t$$
$$g^{n}(a_t, d_t, m_t) = \beta_0 + \beta_1 a_t + \beta_2 d_t + \beta_3 m_t,$$

where the coefficients $\alpha_0, \alpha_1, \alpha_2, \alpha_3, \beta_0, \beta_1, \beta_2, \beta_3$ will differ at each point of the state-space where the local approximation is computed. In Appendix C, we show how expectation operators of equilibrium conditions can be solved in closed form, resulting in large computational gains.

Once we introduce a ZLB into the model the resulting perturbation policies become regime dependent with $j \in \{C, U\}$ denoting constrained or unconstrained:

$$g_j^{\pi}(a_t, d_t, m_t) = \alpha_{0,j} + \alpha_{1,j} a_t + \alpha_{2,j} d_t + \alpha_{3,j} m_t$$
$$g_j^{n}(a_t, d_t, m_t) = \beta_{0,j} + \beta_{1,j} a_t + \beta_{2,j} d_t + \beta_{3,j} m_t,$$

State-Space Representation The states of the model $x_t = (a_t, d_t, m_t)$ are exogenous, so the state-transition equation is not time-varying, with system matrix $T = \text{diag}(\rho_a, \rho_d, \rho_m)$, and $Q = \text{diag}(\sigma_a^2, \sigma_d^2, \sigma_m^2)$ determined by the AR(1) parameters. Assume we observe detrended log output y_t^{obs}, log inflation π_t^{obs}, and log interest rates r_t^{obs}. The observation equation, conditional on the solution at $x = \hat{x}_{t|t-1}$, is:

$$\begin{pmatrix} y_t^{\text{obs}} \\ \pi_t^{\text{obs}} \\ r_t^{\text{obs}} \end{pmatrix} = \begin{pmatrix} \beta_0(x) \\ \pi_{ss} + \alpha_0(x) \\ r_{ss} + \psi_\pi \alpha_0(x) + \psi_y \beta_0(x) \end{pmatrix} + Z(x) \begin{pmatrix} a_t \\ d_t \\ m_t \end{pmatrix} + \varepsilon_t^{ME}, \quad \text{where}$$

$$Z(x) = \begin{pmatrix} \beta_1(x) + 1 & \beta_2(x) & \beta_3(x) \\ \alpha_1(x) & \alpha_2(x) & \alpha_3(x) \\ \psi_\pi \alpha_1(x) + \psi_y(\beta_1(x) + 1) & \psi_\pi \alpha_2(x) + \psi_y \beta_2(x) & \psi_\pi \alpha_3(x) + \psi_y \beta_3(x) + 1 \end{pmatrix},$$

where $\pi_{ss} = \log(\Pi)$ and $r_{ss} = \log(R)$. Note that the bottom row in $Z(x)$ reflects how interest rates depend on both output and inflation through the monetary policy rule $r_t = \psi_\pi \pi_t + \psi_y y_t + m_t$. This linear state-space representation allows us to solve and filter the model as in Algorithm 1.

To filter the model with the ZLB, we assume that it is known to the econometrician when the ZLB episodes take place. In that case, in periods where the ZLB does not bind, one uses the unconstrainted (U) policies, and the state space system above. When the ZLB binds, one uses the constrained (C) policies, and the intercept of the observation equation for r_t^{obs} becomes $-r_{\text{ss}}$ and the row of $Z(x)$ corresponding to r_t^{obs} becomes a row of zeros.

Runtime We use Matlab on a standard laptop without parallelization.[7] We summarize the computation times in Table 3. One thing to note is to get accurate estimates with the particle filter, one needs about a million particles, despite only having three states, making the particle filter computationally costly. This is because the number of particles grows exponentially with the number of states.

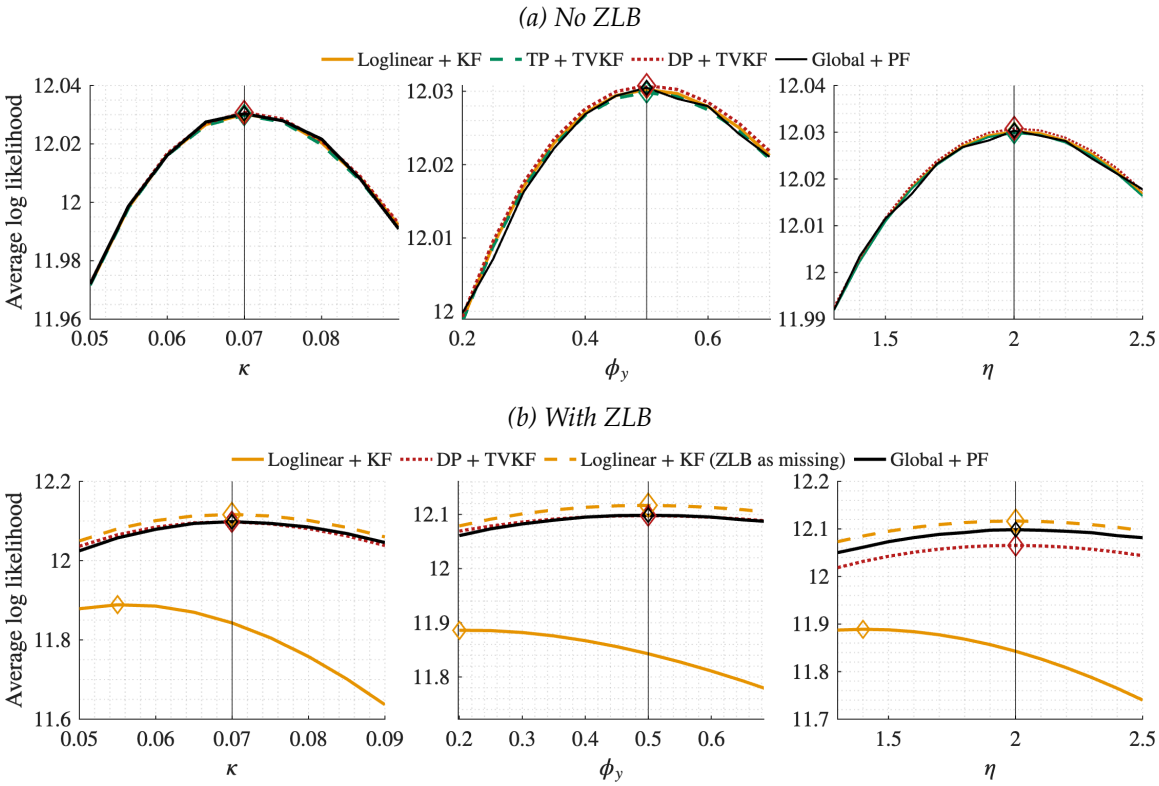
Table 3: Computation time (seconds) for a single likelihood evaluation for $T = 250$.

Method	No ZLB	With ZLB
Loglinear + KF	0.002	0.002
Global + PF (1,000,000)	244.8	248.6
Global + PF (100,000)	24.52	26.10
DP + TVKF	0.002	0.044
TP + TVKF	0.007	—

Comparing Likelihoods As in the previous subsection, Figure 3 compares the likelihoods implied by the different solution methods and filters, for both the model with and without the ZLB. To do so, we simulate a series of length $T = 3{,}000$ from the global model solution. The top row of Figure 3 shows that, for the three-equation New Keynesian model, using a log-linearization introduces no bias, which is unsurprising given that the functional forms make the model essentially log-linear. For the model with the ZLB, however, the log-linear model solution, which ignores the ZLB, generates substantial bias. Interestingly, if one uses the log-linear model and treats the ZLB dates as missing, this bias disappears, but this approach discards approximately 10% of the data. By contrast, dynamic perturbation combined with the time-varying Kalman filter uses all the data and closely matches the likelihood produced by the global method with the particle filter.

[7] Computations are done on a Apple Macbook Pro with an Apple M3 Max processor and 64GB RAM.

Figure 3: Comparing likelihoods for the Phillips curve slope κ, weight on output in the Taylor rule ϕ_y, and inverse Frisch elasticity η in the Three Equation New Keynesian Model



Note: Calibration: $\tau = 1$, $\beta = 0.9971$, $R^{ss} = 1.0088$, $\gamma = 0.1$, $\eta = 2$, $\kappa = 0.07$, $\phi_\pi = 2$, $\phi_y = 0.5$; $\rho_a = 0.85$, $\sigma_a = 0.005$, $\rho_d = 0.92$, $\sigma_d = 0.012$, $\rho_m = 0.7$, $\sigma_m = 0.007$. *Figure compares likelihoods computed based on the time-varying Kalman filter with Dynamic Perturbation and Taylor Projection, the Particle Filter + global model solution, and the linearized model with Kalman filter. Based on a simulation of length* $T = 3000$ *from the global model solution. All other parameters are kept constant at their true values.*

4 A New Keynesian Model with Labor Search

We present a New Keynesian (NK) model with Diamond Mortensen Pissarides (DMP) labor market frictions, where monetary policy transmission depends on firms' flow surplus, leading to state-dependent effects.

4.1 Model

Overview The economy consists of households that consume and supply labor, intermediate-good producers that set prices and hire in a frictional labor market, and final-good producers that aggregate intermediate goods while taking prices as given. Wages are determined by Nash bargaining between the representative

household and intermediate goods firms, and the government sets the nominal interest rate according to an inertial Taylor rule.

Timing We follow the same timing assumption as the DMP model in Section 3. Each period consists of four stages: (i) separations, (ii) search and matching, (iii) bargaining, and (iv) production and consumption/saving.

Households Households are composed of a continuum of members $i \in [0,1]$ who derive utility from consumption $c_t(i)$ and supply one unit of labor $n_t(i) \in \{0,1\}$ if employed. Members perfectly insure each other against income fluctuations. Defining aggregate consumption and employment as $C_t := \int c_t(i)\,di$ and $N_t := \int n_t(i)\,di$, the household maximizes utility:

$$\begin{aligned} & \mathbb{E}_0\left[\sum_{t=0}^{\infty}\beta^t D_t \frac{C_t^{1-\tau}-1}{1-\tau}\right], \\ \text{s.t.} \quad & P_t C_t + B_t = P_t W_t N_t + P_t(1-N_t)b + R_{t-1}B_{t-1} + T_t, \\ & N_t = (1-\delta_t)N_{t-1} + q_t V_t. \end{aligned}$$

Here, β is the discount factor, D_t is a preference shock, $1/\tau$ is the intertemporal elasticity of substitution, P_t is the final good price, B_t are one-period risk-free bonds with gross return R_t, and T_t are lump-sum taxes net of firm profits. W_t is the real wage, b is the value of non-employment, δ_t is the separation rate, V_t is the number of vacancies, and q_t is the vacancy filling rate.

The first-order condition for consumption yields the marginal utility

$$\lambda_t = D_t C_t^{-\tau},$$

and the stochastic discount factor is given by

$$Q_{t,t+1} = \beta\frac{\lambda_{t+1}}{\lambda_t}.$$

The saving Euler equations is:

$$1 = \beta\mathbb{E}_t\left[R_t\frac{D_{t+1}}{D_t}\left(\frac{C_{t+1}}{C_t}\right)^{-\tau}\frac{P_t}{P_{t+1}}\right] = \mathbb{E}_t\left[Q_{t,t+1}\frac{R_t}{\Pi_{t+1}}\right],$$

where $\Pi_t = P_t/P_{t-1}$ is inflation. The household surplus from employment, using the envelope condition, is

$$S_t^h = W_t - b + \mathbb{E}_t \left[Q_{t,t+1}(1-\delta_{t+1}) S_{t+1}^h \right],$$

representing the present value of a marginal employed household member.

Search and Matching Aggregate hires are determined by a constant-returns-to-scale matching function $M_t = A_t M(V_t, S_t)$, where A_t is matching efficiency, V_t is the number of vacancies, and S_t is the mass of unmatched workers. Given the timing, unmatched workers are given by:

$$S_t = 1 - (1-\delta_t) N_{t-1},$$

which includes workers who were not matched previously and those who separated at the start of the period. Market tightness is defined as $\Theta_t = V_t/S_t$, and the vacancy filling rate is:

$$q_t = \frac{M_t}{V_t} = A_t M\left(1, \Theta_t^{-1}\right).$$

Final Goods Producers Final-good producers aggregate intermediate goods $Y_t(j)$, $j \in [0,1]$, using a CES aggregator:

$$Y_t = \left(\int_0^1 Y_t(j)^{1-\gamma} dj \right)^{\frac{1}{1-\gamma}}.$$

They take input and output prices as given and maximize profits. Optimality implies the demand for good j:

$$Y_t(j) = \left(\frac{P_t(j)}{P_t} \right)^{-\frac{1}{\gamma}} Y_t.$$

Intermediate Goods Producers A continuum of identical monopolistic producers $j \in [0,1]$ produces using the linear technology

$$Y_t(j) = Z_t N_t(j),$$

where Z_t is aggregate productivity. Firms face quadratic Rotemberg price adjustment costs,

$$AC_t(j) = \frac{\phi}{2}\left(\frac{P_t(j)}{P_{t-1}(j)} - \Pi\right)^2 Y_t,$$

and hire labor in frictional markets by posting vacancies at cost c. Each firm chooses $N_t(j)$, $V_t(j)$, and $P_t(j)$ to maximize:

$$\Pi_0(j) = \mathbb{E}_0 \sum_{t=0}^{\infty} Q_{0,t}\left[\left(\frac{P_t(j)}{P_t} Z_t - W_t\right) N_t(j) - cV_t(j) - AC_t(j)\right],$$

subject to:

$$Z_t N_t(j) = \left(\frac{P_t(j)}{P_t}\right)^{-\frac{1}{\gamma}} Y_t, \quad [\omega_t]$$
$$N_t(j) = (1-\delta_t)N_{t-1}(j) + q_t V_t(j). \quad [\mu_t]$$

The multiplier ω_t captures the implicit cost of hiring due to downward movement on the demand curve, while μ_t denotes the marginal value of employment to the firm.

Wage Bargaining The wage is determined by the Nash sharing rule

$$\eta \mu_t = (1-\eta) S_t^h,$$

where η is the worker's bargaining weight. This implies the real wage is

$$W_t = \eta(1-\omega_t)Z_t + (1-\eta)b,$$

where b is the flow value of non-employment and ω_t is the implicit marginal cost of hiring.

Government Monetary policy is determined by a Taylor rule for the nominal interest rate:

$$R_t = R\left(\frac{\Pi_t}{\Pi}\right)^{\phi_\pi}\left(\frac{Y_t}{Y}\right)^{\phi_y},$$

where R_t is the systematic component of the policy rule and m_t is an inertial monetary policy shock, $\Pi_t = P_t/P_{t-1}$ is inflation and Y_t is output. The government balances the budget period by period using lump-sum taxes or transfers.

Exogenous States The discount factor, $d_t = \ln D_t$, productivity, $z_t = \ln Z_t$, and the monetary policy shock, m_t, follow AR(1) processes in logs. The separation rate, $\delta_t = \delta e^{s_t}$, and the matching efficiency, $A_t = Ae^{a_t}$, also include log-linear stochastic components that follow AR(1) processes:

$$z_t = \rho_z z_{t-1} + \sigma_z \varepsilon_t^z, \quad d_t = \rho_d d_{t-1} + \sigma_d \varepsilon_t^d, \quad m_t = \rho_m m_{t-1} + \sigma_m \varepsilon_t^m,$$
$$s_t = \rho_s s_{t-1} + \sigma_s \varepsilon_t^s, \quad a_t = \rho_a a_{t-1} + \sigma_a \varepsilon_t^a.$$

Equilibrium Conditions We assume that vacancy posting and price adjustment costs are rebated to households in lump sum, so market clearing implies:

$$C_t = Y_t = Z_t N_t.$$

The household Euler equation becomes:

$$1 = \beta \mathbb{E}_t \left[\frac{D_{t+1}}{D_t} \left(\frac{Y_{t+1}}{Y_t} \right)^{-\tau} \frac{R_t}{\Pi_{t+1}} \right].$$

In a symmetric equilibrium, all firms set the same price $P_t = P_t(j)$ and choose the same level of employment $N_t(j) = N_t$ and vacancies $V_t(j) = V_t$, which yields the pricing equation:

$$\frac{\omega_t}{\gamma} = 1 - \phi(\Pi_t - \Pi)\Pi_t + \phi\beta \mathbb{E}_t \left[\frac{D_{t+1}}{D_t} \left(\frac{Y_{t+1}}{Y_t} \right)^{1-\tau} (\Pi_{t+1} - \Pi)\Pi_{t+1} \right].$$

Combining the vacancy posting condition with the Nash wage expression yields the job-creation condition:

$$\frac{c}{q_t} = (1-\eta)\left[(1-\omega_t)Z_t - b\right] + \beta \mathbb{E}_t \left[(1-\delta_{t+1}) \frac{D_{t+1}}{D_t} \left(\frac{Y_{t+1}}{Y_t} \right)^{-\tau} \frac{c}{q_{t+1}} \right].$$

The Taylor rule for the nominal interest rate and the law of motion for employment complete the system. The model admits a minimum state variable rep-

resentation with state vector $x_t = (N_{t-1}, z_t, d_t, m_t, s_t, a_t)$, and policy functions $\{\Pi(x_t), \omega(x_t), \theta(x_t)\}$.

4.2 State Dependence

The quantitative results section will examine the state-dependent effects of monetary policy shocks. As a preliminary step, analyzing the log-linearized system helps clarify the model's propagation mechanisms.

We study the perfect foresight response to a one-time monetary policy shock, $\varepsilon_0^m = 1$, $\varepsilon_t^m = 0 \ \forall t > 0$, using the log-linearized system. Focusing on two key equations:

$$\text{Phillips curve:} \quad \hat{\pi}_t = \beta \hat{\pi}_{t+1} - \frac{1}{\phi}\hat{\omega}_t$$

$$\text{Job creation:} \quad \hat{q}_t = \frac{\gamma(1-\beta(1-\delta))}{(1-\eta)(1-\gamma-b)}\hat{\omega}_t + (1-\delta)\beta\left[\hat{q}_{t+1} + \hat{r}_t - \hat{\pi}_{t+1}\right]$$

The job-creation condition shows that the sensitivity of the vacancy-filling rate (i.e., market tightness) $\hat{q}_t$ to a cost shock $\hat{\omega}_t$ increases as steady-state flow profits, given by $(1-\eta)(1-\gamma-b)$, decline. This mechanism relates to the fundamental surplus concept in Ljungqvist and Sargent (2017), but here in the context of monetary policy. Smaller flow profits amplify the effect of a monetary shock on market tightness, employment, and output. Since $\hat{\pi}_t$ loads on $\hat{\omega}_t$ in the Phillips curve, this channel also governs the inflation response. The degree of price stickiness, ϕ, determines the strength of this pass-through.

In the log-linearized NK-DMP model, elasticities to shocks are constant and pinned down by steady-state values. In contrast, a nonlinear solution allows flow profits to vary with the state, generating state-dependent monetary policy transmission.

4.3 Solution and Estimation

We solve the model locally by expressing states and policies as log-deviations from their steady-state values, e.g., $\theta_t = \ln(\Theta_t/\Theta)$ and $z_t = \ln(Z_t/Z)$. We assume the law of motion for employment n_t, and policy functions for inflation π_t, marginal cost ω_t, and market tightness θ_t are linear in the state vector $x_t = \{n_{t-1}, z_t, d_t, m_t, s_t, a_t\}$.

This yields the following linear functions:

$$\theta_t = b_0^\theta + B^\theta x_t, \qquad \pi_t = b_0^\pi + B^\pi x_t,$$
$$\omega_t = b_0^\omega + B^\omega x_t, \qquad n_t = b_0^n + B^n x_t,$$

where each B_x^i is a 1×6 vector. Expectations in the equilibrium system can be solved in closed form (see Appendix D), and coefficients are recovered using both the Taylor projection and dynamic perturbation methods.

We map the model to data using six observables: market tightness θ_t^{obs}, the separation rate s_t^{obs}, employment n_t^{obs}, inflation (GDP deflator) $\pi_t^{1,\text{obs}}$, inflation $\pi_t^{2,\text{obs}}$ (CPI) and the Federal Funds rate r_t^{obs}. Measurement equations incorporate error:

$$\pi_t^{i,\text{obs}} = \pi_{ss} + \pi_t + \sigma_{\pi,i}^{ME}\varepsilon_t^{\pi,i}, \qquad i = 1,2$$
$$n_t^{\text{obs}} = n_t + \sigma_n^{ME}\varepsilon_t^n, \qquad \theta_t^{\text{obs}} = \theta_t + \sigma_\theta^{ME}\varepsilon_t^\theta,$$
$$r_t^{\text{obs}} = r_{ss} + r_t + \sigma_r^{ME}\varepsilon_t^r, \qquad s_t^{\text{obs}} = s_t + \sigma_s^{ME}\varepsilon_t^s,$$

Letting $y_t^{1,\text{obs}} = (\pi_t^{2,\text{obs}}, \pi_t^{\text{obs}}, n_t^{\text{obs}}, \theta_t^{\text{obs}}, r_t^{\text{obs}}, s_t^{\text{obs}})'$, and solving the model at $x = \hat{x}_{t|t-1}$, the state-space system matrices become:

$$d_t = \begin{pmatrix} \pi_{ss} + b_0^\pi(x) \\ \pi_{ss} + b_0^\pi(x) \\ 0 \\ b_0^\theta(x) \\ r_{ss} + b_0^r(x) \\ 0 \end{pmatrix}, \; Z_t = \begin{pmatrix} B^\pi(x) \\ B^\pi(x) \\ 1\ 0\ 0\ 0\ 0\ 0 \\ B^\theta(x) \\ B^r(x) \\ 0\ 0\ 0\ 0\ 1\ 0 \end{pmatrix}, \; c_t = \begin{pmatrix} b_0^n(x) \\ 0 \\ 0 \\ 0 \\ 0 \\ 0 \end{pmatrix}, \; T_t = \begin{pmatrix} B^n(x) \\ 0\ \rho_z\ 0\ 0\ 0\ 0 \\ 0\ 0\ \rho_d\ 0\ 0\ 0 \\ 0\ 0\ 0\ \rho_m\ 0\ 0 \\ 0\ 0\ 0\ 0\ \rho_s\ 0 \\ 0\ 0\ 0\ 0\ 0\ \rho_a \end{pmatrix}.$$

We estimate the model using full-information Bayesian methods over the 1984:Q1 – 2007:Q4 sample, that is, post Great-moderation and pre-ZLB. Appendix Table B1 summarizes the data and transformations.

4.4 Empirical Framework: State-Dependent Local Projections

While the model yields state-dependent responses to monetary shocks by imposing a full structural framework, it remains an open question whether such state dependence is present in the data without structural restrictions. To address this, we

turn to model-free reduced-form evidence to assess whether such state-dependent effects are empirically relevant. We use the state-dependent local projection (LP) approach of Cloyne et al. (2023), which extends Jordà (2005). For a policy shock s_t and state variable x_t, we estimate:

$$y_{t+h} = \alpha_h + \beta_h s_t + \beta_h^x s_t(x_t - \bar{x}) + w_t\gamma_h + \varepsilon_t, \quad h = 0, \ldots, H, \tag{41}$$

where w_t includes controls. The state-dependent response is $\hat{\beta}_h + \hat{\beta}_h^x(x_t - \bar{x})$. We estimate the model using IV, interacting the shock and state with external instruments. While causal interpretation requires exogeneity (Gonçalves et al., 2023), our goal is to show this reduced-form evidence coincides with our model output.

Outcomes variables include unemployment, market tightness, CPI, and vacancies, using JOLTS and the Help-Wanted Index from Barnichon (2010) pre-2001. Controls include CPI, unemployment, PPI, the excess bond premium, and 12 lags of policy and outcome variables (as in Bauer and Swanson, 2023). As a proxy for the state, we use the unemployment rate. As the shock series, we use the narrative shocks of Romer and Romer (2004) (extended by Wieland and Yang 2020).

5 Model Results

We present quantitative results from the model solved via Taylor projections, using a time-varying Kalman filter to infer latent states. This approach yields time-varying impulse response functions and other policy-relevant objects, enabling a quantification of state-dependent monetary policy transmission.

5.1 Parameter Estimates

Some parameters are calibrated (Table 4), while the remaining parameters are estimated in a Bayesian framework using a Random-Walk Metropolis–Hastings (RWMH) sampler; priors and posterior estimates are reported in Table 5. The table also reports computation times, and shows that it would take approximately 25 minutes to obtain 100,000 draws from a RWMH sampler using Dynamic Perturbation + TV-KF. All three solution methods—log-linear + KF, Taylor projection + TVKF, and dynamic perturbation + TVKF—are estimated on the common sample 1984Q1–2007Q4.

The resulting parameter estimates are generally quite similar across methods. The main difference is that the log-linear specification implies a substantially larger measurement error for market tightness than the other two approaches. This is consistent with the fact that the key nonlinearity in the model stems from the job-creation condition: the log-linear approximation appears to match the data with similar structural parameters, but at the cost of attributing more of the discrepancy to measurement error in market tightness.

Table 4: Calibrated parameters

Parameter	Calibrated value
η: bargaining weight	0.5
τ: risk aversion	2
γ: inverse elasticity of substitution CES aggregator	0.1
q_{ss}: steady state vacancy-filling rate	0.6
θ_{ss}: steady state market tightness	1
n_{ss}: steady state employment	0.945
δ: exogenous job destruction rate	$\frac{q_{ss}\theta_{ss}(1-n_{ss})}{(1-q_{ss}\theta_{ss})n_{ss}}$
s_{ss}: steady state separation rate	$\log \delta$
a_{ss}: steady state match efficiency	$\log q_{ss}$
c: vacancy cost	$\frac{(1-\eta)(1-\gamma-\nu)q_{ss}}{1-\beta(1-\delta)}$

Figure 4: State-Dependent Policy Coefficients for DP (no ZLB), computed at filtered states

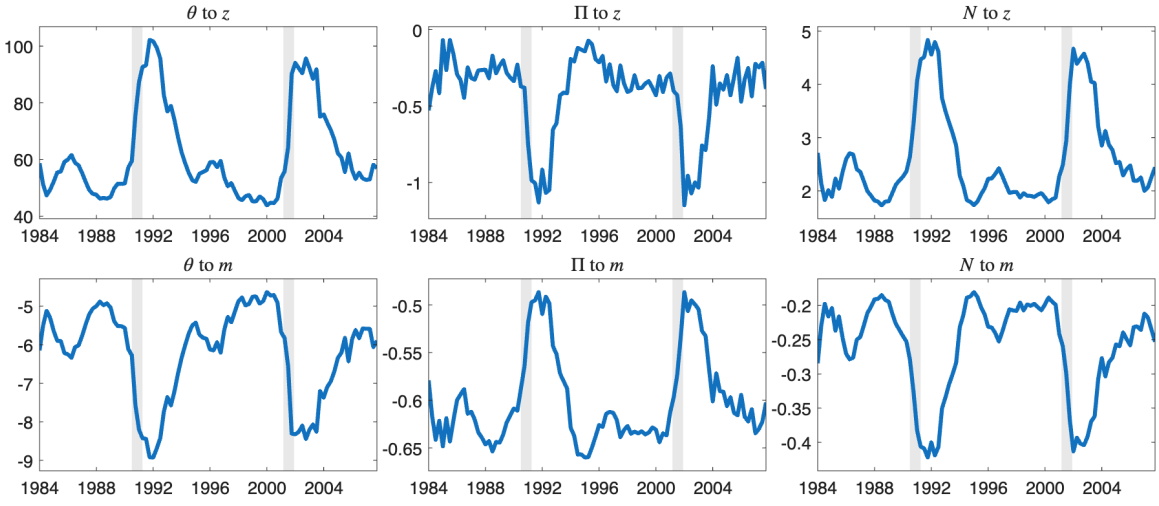


Table 5: Prior distributions (reported by mean and standard deviation) and posterior means with standard deviations for the log-linear, DP+TV-KF, and TP+TV-KF specifications. The estimation sample is 1984Q1–2007Q4 for all methods.

Parameter	Prior Distr.	Posterior		
	(Mean, Std.)	Log-linear	DP+TV-KF	TP+TV-KF
Economic parameters				
κ: slope Phillips curve	B(0.15, 0.02)[a]	0.08 (0.02)	0.08 (0.02)	0.10 (0.02)
ϕ_π: inflation Taylor rule	G(1.75, 0.10)[b]	1.87 (0.08)	1.88 (0.09)	1.83 (0.09)
ϕ_y: output Taylor rule	G(0.50, 0.10)	0.24 (0.03)	0.22 (0.03)	0.23 (0.03)
ν^*: normalized flow value unemployment	B(0.90, 0.02)	0.98 (0.01)	0.98 (0.00)	0.98 (0.01)
Exogenous process parameters				
$100 \times \sigma_z$: std. TFP shocks	IG(1.00, 2.00)	0.22 (0.05)	0.23 (0.05)	0.25 (0.06)
$100 \times \sigma_d$: std. DF shocks	IG(1.00, 2.00)	0.65 (0.14)	0.66 (0.16)	0.72 (0.17)
$100 \times \sigma_s$: std. separation shocks	IG(1.00, 2.00)	4.62 (0.35)	4.59 (0.36)	4.50 (0.32)
$100 \times \sigma_m$: std. MP shocks	IG(1.00, 2.00)	0.30 (0.03)	0.30 (0.03)	0.29 (0.03)
$100 \times \sigma_a$: std. matching efficiency shocks	IG(1.00, 2.00)	3.58 (0.30)	3.71 (0.32)	3.48 (0.30)
ρ_z: persistence TFP	B(0.50, 0.15)	0.97 (0.01)	0.97 (0.01)	0.98 (0.00)
ρ_d: persistence DF	B(0.50, 0.15)	0.86 (0.03)	0.86 (0.03)	0.85 (0.04)
ρ_s: persistence separations	B(0.50, 0.15)	0.87 (0.02)	0.87 (0.02)	0.87 (0.02)
ρ_m: persistence monetary policy	B(0.50, 0.05)	0.58 (0.04)	0.57 (0.04)	0.59 (0.04)
ρ_a: persistence matching efficiency	B(0.50, 0.15)	0.84 (0.02)	0.84 (0.02)	0.87 (0.01)
Measurement error				
$100 \times \sigma_{\pi_1}^{ME}$: ME GDP Deflator	IG(0.50, 5.00)	0.06 (0.01)	0.06 (0.01)	0.06 (0.01)
$100 \times \sigma_{\pi_2}^{ME}$: ME CPI Inflation	IG(0.50, 5.00)	0.31 (0.02)	0.31 (0.02)	0.31 (0.03)
$100 \times \sigma_N^{ME}$: ME employment	IG(0.50, 5.00)	0.11 (0.03)	0.13 (0.02)	0.14 (0.02)
$100 \times \sigma_Q^{ME}$: ME tightness	IG(0.50, 5.00)	1.88 (0.71)	0.15 (0.07)	0.13 (0.07)
$100 \times \sigma_r^{ME}$: ME FFR	IG(0.50, 5.00)	0.06 (0.01)	0.06 (0.01)	0.07 (0.01)
$100 \times \sigma_s^{ME}$: ME separations	IG(0.50, 5.00)	0.29 (0.27)	0.29 (0.30)	0.51 (0.54)
Log posterior kernel at posterior mean		1952.7	1961.5	1945.5
Computation time (seconds, 1000 likelihood evals.)		1.3	14.1	24.6

Notes: [a] *The prior for κ is a Beta prior truncated from below at 0.005.* [b] *The prior for ϕ_π is a shifted Gamma prior with support on $\phi_\pi > 1$. B denotes Beta, G Gamma, and IG Inverse Gamma. The reported posterior for ν^* refers to the normalized parameter estimated in the sampler; the model-implied flow value is $\nu = \nu^*(1 - \gamma - 0.01)$.*

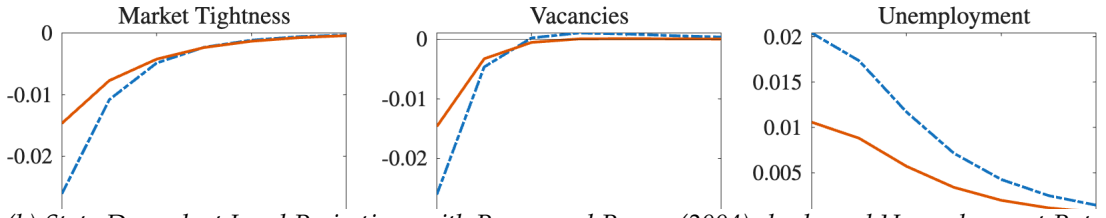
5.2 Time-Varying Impulse Responses

A key feature of the method is that it solves the model at each point in time. Shock propagation varies with the underlying state of the economy through the local policy coefficients, which are constant in a log-linearized model. Figure 4 plots a subset of these policy coefficients with 68% credible intervals. Since all variables are in log-deviations from steady state, these coefficients are elasticities. They vary systematically: the elasticities of market tightness, inflation and employment to productivity and monetary policy shocks increase in absolute value during recessions when surplus is small.

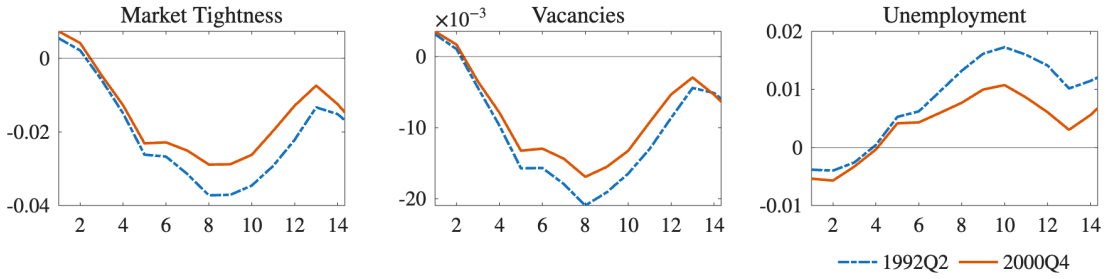
Time-variation in policy rules leads to time variation in impulse responses, shown in Figure 5 for unemployment, market tightness, and vacancies at two dates based on filtered states: 2000Q4 (high-surplus, weak propagation) and 1992Q2 (low-surplus, strong propagation). We compare model-implied IRFs to those implied by state-dependent local projections. The model IRFs are comparable with the local projections for unemployment, vacancies and market tightness, though they lack hump-shaped dynamics which would require additional model features like habit formation.

Figure 5: Impulse Response Functions over Time: 1992Q2 (blue dash-dot) and 2000Q4 (red solid)

(a) Nonlinear model (Dynamic Perturbation – No ZLB)



(b) State-Dependent Local Projections with Romer and Romer (2004) shocks and Unemployment Rate State Proxy



5.3 Phillips Multiplier

A key concern for policymakers is the unemployment-inflation trade-off, which captures the nominal effects relative to the real effects of a monetary policy shock. However, state dependence in impulse responses alone does not necessarily imply variation in the unemployment-inflation trade-off; this depends on whether the real versus nominal effects differ in relative magnitude across states. To illustrate that the unemployment-inflation trade-off is state dependent, we use the concept of the Phillips Multiplier (PM), as in Barnichon and Mesters (2021), motivated by Mankiw (2001). The PM quantifies this trade-off by measuring the average change in inflation caused by an interest rate change that reduces the unemployment rate by one percentage point over h periods:

$$T_h = \frac{\partial \bar{\Pi}_{t:t+h}}{\partial R_t}\Big|_{\varepsilon_t} \Big/ \frac{\partial \bar{U}_{t:t+h}}{\partial R_t}\Big|_{\varepsilon_t}$$

Here $\bar{\Pi}_{t:t+h}$ is the average over variable Π over h time periods, and ε_t is the exogenous change in the interest rates. The statistical counterpart of T_h is the PM:

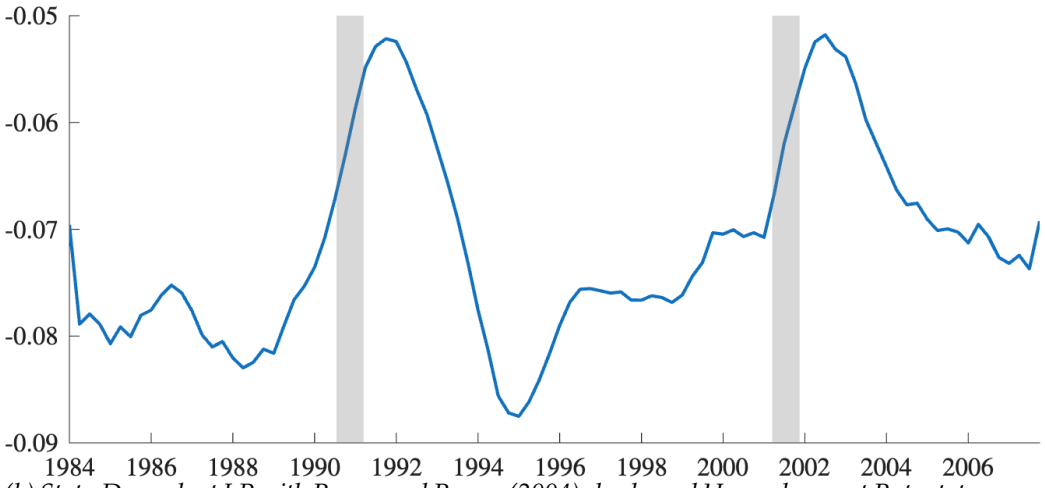
$$\mathcal{P}_h = \mathcal{R}_h^{\bar{\Pi}} / \mathcal{R}_h^{\bar{U}}, \quad h = 0, 1, 2, ...,$$

that is, the ratio of the cumulative impulse response function (up to horizon h) of inflation over unemployment. We use h is 16 quarters.

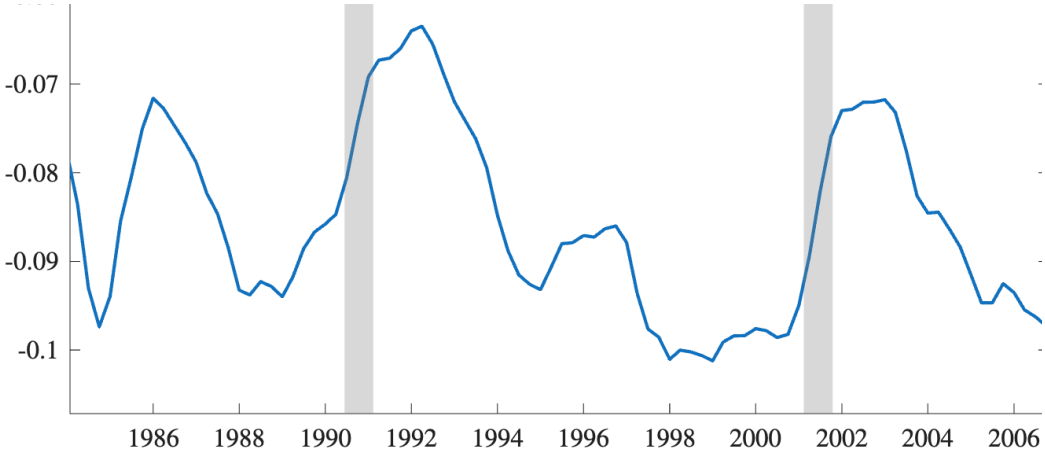
We compute time-varying impulse responses to monetary policy shocks using the model's filtered states to construct a PM series and validate these results with the state-dependent local projections using unemployment as a proxy. Figure 6 shows the PM for our estimation sample. The PM ranges between -0.09 and -0.05 in both the model and the data, and is countercyclical – flattening in recessions and steepening during expansions.

Figure 6: Time-variation in the Phillips Multiplier

(a) Nonlinear model (DP no ZLB) – nonlinear parameter estimates



(b) State-Dependent LP with Romer and Romer (2004) shocks and Unemployment Rate state proxy



6 Extensions

This section considers three extensions that our framework can accommodate.

6.1 Stochastic Volatility

A common extension of DSGE models introduces time-varying volatility in exogenous shocks, typically modeled as stochastic volatility (SV). For instance, total factor productivity z_t may follow:

$$z_t = \rho_z z_{t-1} + e^{\xi_t/2} u_t, \quad \xi_t = (1 - \rho_\xi)\mu_\xi + \rho_\xi \xi_{t-1} + v_t,$$

where ξ_t governs the volatility of u_t and follows an AR(1) process with Gaussian innovations. In this case, the state vector x_t is augmented to include ξ_t. In Appendix E, we show how the Taylor Projection method accommodates SV, using a stochastic growth model as an example. Unlike perturbation methods, which require higher-order expansions to capture risk effects, Taylor Projection yields non-certainty-equivalent linear policy rules that load directly on the volatility state.

Stochastic volatility complicates filtering due to the nonlinear transition equation:

$$x_t = T x_{t-1} + c + R(x_t)\eta_t,$$

where $R(x_t)$ depends on the state, preventing the use of a standard Kalman filter. In Appendix E, we discuss two approaches: (i) the Extended Kalman Filter (EKF), which linearizes $R(x_t)$ around $\hat{x}_{t|t-1}$, or (ii) discretization of ξ_t using finite-state Markov-chain approximations, yielding a discrete process $\tilde{\xi}_t$. Conditional on $\tilde{\xi}_t$, the system is linear and allows for Kalman filtering, while $\tilde{\xi}_t$ itself is filtered using the Hamilton (1994) filter. This approach is related to Friedman and Harris (1998).

6.2 Regime Switching or Rare Disasters

Another common extension is the regime-switching DSGE model, e.g., Liu et al. (2011), which underlies frameworks such as the rare disaster model (Barro, 2009). Here, the exogenous process departs from a stationary VAR(1), with dynamics instead governed by a latent discrete state $s_t \in \{0, \ldots, S\}$ evolving via a Markov

chain with transition matrix Π:

$$x_{2,t} = A(s_t)x_{2,t-1} + B(s_t)\eta_t, \quad \text{where} \quad s_t \sim \Pi.$$

In Appendix E, we show how the Taylor Projection method can accommodate regime switching by assigning regime-specific local linear policy functions, $y_t = g_{s,x}(x_t)$, and transition functions, $x_{t+1} = h_{s,x}(x_t)$ for each $s \in \{0, \ldots, S\}$ where the subscripts indicate the policy rules depend on both regime s and states x. Agents form expectations accounting for regime-dependent shifts in policy rules. The resulting model has a linear state-space representation conditional on regime s_t, allowing likelihood evaluation via the Kalman filter. The latent regime s_t is inferred using the Hamilton (1994) filter, making the filtering step exact.

6.3 Heterogeneous agents

Recall the notation for a standard Dynamic Stochastic General Equilibrium (DSGE) model in Equation (1):

$$\mathbb{E}_t \left[f(y_{t+1}, y_t, x_{t+1}, x_t) \right] = 0.$$

Heterogeneous agent models can also be written in this form, but the key challenge is that the state vector x_t includes an infinite-dimensional object: a measure μ_t over all idiosyncratic states. For example, in the heterogeneous household model of Krusell and Smith (1998), μ_t is the joint distribution over individual assets a and idiosyncratic efficiency units of labor ε. A common solution is to approximate μ_t using a finite-dimensional object. Examples include histograms (Reiter, 2009), or moment-based polynomial expansions (Winberry, 2018).

For illustration, we focus on a simple heterogeneous household model; a detailed description is provided in Appendix F. In brief, the model features households $i \in [0, 1]$ with preferences over consumption c_{it}, represented by

$$\mathbb{E}_t \sum_{t=0}^{\infty} \beta^t \frac{c_{it}^{1-\sigma} - 1}{1 - \sigma},$$

where β is the discount factor and $1/\sigma$ is the intertemporal elasticity of substitution. Households supply labor inelastically with employment status $\varepsilon_{it} \in \{0, 1\}$ (unemployed or employed) varying stochastically, and receive income $w_t[(1-\tau_t)\varepsilon_{it} + b(1-$

$\varepsilon_{it})$], where w_t is the wage, τ_t the labor tax rate, and b denotes the replacement rate of unemployment benefits. Assuming a balanced government budget in every period implies that the labor income tax rate satisfies $\tau_t = b(1 - L_t)/L_t$, where L_t is the aggregate employment rate. Households save in uncontingent assets a_{t+1} earning a return r_t, subject to a borrowing constraint $a_{t+1} \geq 0$. The probability of finding employment $f_t = p(\varepsilon_{i,t+1} = 1|\varepsilon_{i,t} = 0)$ and separating into unemployment $s_t = p(\varepsilon_{i,t+1} = 0|\varepsilon_{it} = 1)$ are given by:

$$f_t = \bar{f} e^{\eta_f z_t}, \;\; s_t = \bar{s} e^{\eta_s z_t},$$

where η_f and η_s are parameters, and z_t is aggregate productivity (TFP), evolving as an AR(1). This implies aggregate employment L_t follows the law of motion:

$$L_{t+1} = f_t(1 - L_t) + s_t L_t.$$

Within this model environment, employment transitions depend on the aggregate state, making recessions periods of heightened unemployment risk (as in Krueger et al., 2016), leading to time-varying precautionary saving motives.

A representative firm produces output using capital and labor $Y_t = e^{z_t} K_t^{\alpha} L_t^{1-\alpha}$, with α the capital share. Capital depreciates at rate δ. The firm maximizes profits so that factors are paid their marginal products r_t and w_t, respectively. The model is closed by market-clearing conditions that equate aggregate capital demand and supply. Since prices depend on the cross-sectional distribution of assets and employment, μ_t enters the equilibrium conditions, requiring households to forecast this distribution. As a result, μ_t is a state variable. Similar to Winberry (2018), we approximate μ_t, which is infinite-dimensional, with the maximum entropy distribution:

$$\mu_{\varepsilon,t}(a) \approx g^0_{\varepsilon,t} \exp\left\{ \sum_{i=1}^{n_g} g^i_{\varepsilon,t} a^i \right\}, \text{ for } \varepsilon \in \{0, 1\}, \tag{42}$$

with $\mathbf{g}_t$ coefficients, chosen by matching a finite set of moments $\mathbf{m}_t$.

In addition to approximating the cross-sectional distribution μ_t, to map this model into a standard DSGE model form, we need to approximate the decision rules of the household, which follow from the household Euler equation and the borrowing

constraint. Following Winberry (2018), we approximate the expected marginal utility from saving using Chebychev polynomials:

$$\mathbb{E}\left[\beta(1+r_{t+1})c_{t+1}(\varepsilon', a_t'(\varepsilon, a))^{-\sigma}\right] \approx \exp\left\{\sum_{j=1}^{n_\psi} \theta^j_{\varepsilon,t} T_{j-1}(\xi(a))\right\}, \tag{43}$$

with n_ψ the number of Chebychev nodes, T_j denotes the jth-order Chebychev polynomial, $\theta^j_{\varepsilon,t}$ are the coefficients, and $\xi(a) = 2\frac{a-\underline{a}}{\bar{a}-\underline{a}} - 1$. The approximation (43) holds exactly at Chebychev nodes $\{a_j\}_{j=1}^{n_\psi}$.

This results in a minimal state-space representation of the heterogeneous household model with state vector $x_t \equiv (z_t, \mathbf{m}_t, L_t)$ and controls $y_t \equiv (\boldsymbol{\theta}_t, \mathbf{g}_t)$. The equilibrium conditions take the form of Equation (1), with the full system detailed in Appendix F. Rather than perturbing this system (Winberry, 2018; Reiter, 2009) or solving it under perfect foresight (Auclert et al., 2021), we use Taylor Projections. In what follows, when states and policies are expressed in log-deviations from steady state, they are denoted by $\hat{\cdot}$, and $\bar{\cdot}$ denotes a steady state value. In the Taylor Projection approach, we use two moments to approximate the cross-sectional distribution $\mu_{\varepsilon,t}(a)$, so the local linear policy functions take the form:

$$\begin{aligned}
\mathbf{g}_t &= \bar{\mathbf{g}} + b_0^g + B^g \begin{bmatrix} \hat{z}_t & m^1_{0,t} & m^1_{1,t} & m^2_{0,t} & m^2_{1,t} \end{bmatrix}' \\
\boldsymbol{\theta}_t &= \bar{\boldsymbol{\theta}} + b_0^\theta + B^\theta \begin{bmatrix} \hat{z}_t & m^1_{0,t} & m^1_{1,t} & m^2_{0,t} & m^2_{1,t} \end{bmatrix}',
\end{aligned}$$

where $\mathbf{g}_t$ and $\boldsymbol{\theta}_t$ are vectors, so B^g and B^θ are matrices. Note, these equations are of the form $y_t = \bar{y} + B \times (1, x_t)'$, such that the Taylor projection is centered at the steady state value when $B = 0$. Thus, the unknown policies are linear deviations from the steady-state value. In addition to the local linear policy rules, the Taylor Projection solution yields linearized laws of motions for endogenous states, i.e., moments $i = 1, 2$, $\varepsilon \in \{0, 1\}$, and aggregate employment:

$$m^i_{\varepsilon,t+1} = \bar{m}^i_\varepsilon + b_0^{m,\varepsilon,i} + B^{m,\varepsilon,i} \begin{bmatrix} \hat{z}_t & m^1_{0,t} & m^1_{1,t} & m^2_{0,t} & m^2_{1,t} & L_t \end{bmatrix}', \tag{44}$$

$$L_{t+1} = \bar{L} + b_0^L + B^L \begin{bmatrix} \hat{z}_t & m^1_{0,t} & m^1_{1,t} & m^2_{0,t} & m^2_{1,t} & L_t \end{bmatrix}'. \tag{45}$$

Under dynamic Taylor Projection, solving the model locally at different points in the state space yields different policy coefficients, allowing the solution to capture state dependence with respect to the current aggregate state x_t. Such state dependence has been shown to be empirically relevant. For instance, in heterogeneous firm models, Ottonello and Winberry (2020) argue that monetary policy transmission varies with the distribution of firms' distance to default. Dynamic Taylor Projections can accommodate this type of state-dependent shock transmission.

In Appendix F we derive the approximate linear mapping of output $\hat{Y}_t = \ln(Y_t/\bar{Y})$ to states. This allows us to map the model into a linear state space form. The state transition equation follows from Equation (44)-(45) and $\hat{z}_t$ being an AR(1). For the measurement equation, assume, for example, that we observe deviations of aggregate output. Then, our measurement equation is given by

$$y_t^{\text{obs}} = b_0^y + B^y \begin{bmatrix} \hat{z}_t & m_{0,t}^1 & m_{1,t}^1 & m_{0,t}^2 & m_{1,t}^2 & L_t \end{bmatrix}' + \varepsilon_t^{\text{ME}}, \quad \varepsilon_t^{\text{ME}} \sim N(0, Q).$$

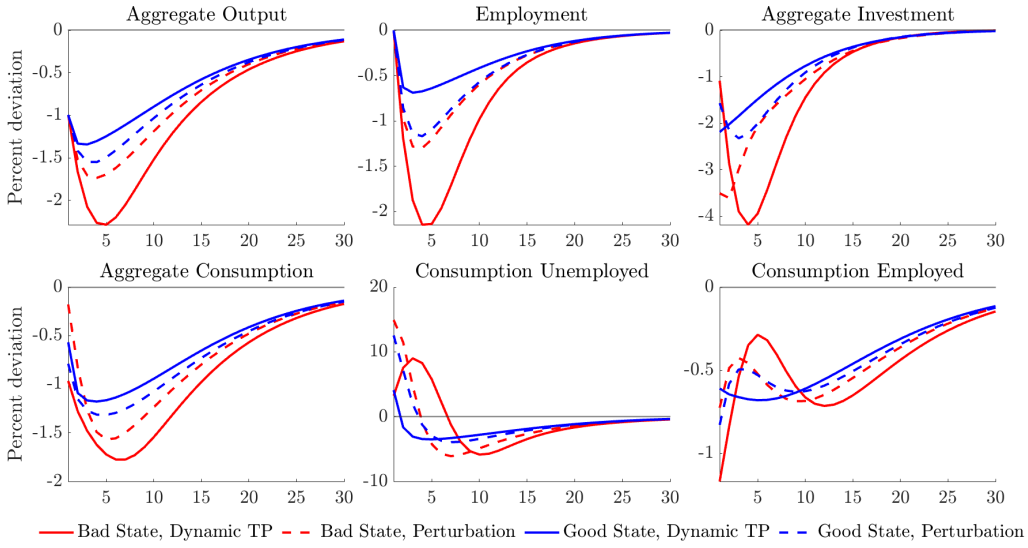
It is also possible to incorporate micro-level data, such as repeated cross-sections, into the estimation procedure, following the approach in Liu and Plagborg-Møller (2023). This involves evaluating the cross-sectional data points using the density in Equation (42) evaluated at many draws from the model-implied distribution of the smoothed states $\mathbf{m}_t$ and $\mathbf{g}_t$. The resulting micro log-likelihood can then be combined with the macro log-likelihood derived from the filtered states.

State Dependence We use the dynamic Taylor Projection (TP) method to show that even a relatively simple heterogeneous household model exhibits nonlinearities that standard perturbation methods fail to capture. We compare impulse response functions from the TP and perturbation-based solutions,[8] evaluating responses to a one-standard-deviation negative TFP shock under two initial conditions: (i) a *good* state (TFP one standard deviation above steady state for five periods) and (ii) a *bad* state (TFP one standard deviation below). As shown in Figure 7, perturbation significantly understates state dependence. Impulse response functions differ not only in magnitude but also in shape and timing. For example, TP produces a hump-shaped investment response only in the bad state, while perturbation predicts a similar response in both. Similar discrepancies arise in

[8] Following Levintal (2018), first-order TP converges to a perturbation solution as $\sigma_z \to 0$.

the consumption paths of employed and unemployed households. Appendix F further shows that sign-dependence in shock transmission is similarly understated by perturbation.

Figure 7: State-Dependence in a Heterogeneous Household Model: Perturbation versus Dynamic Taylor Projection



Comparing Filters We compare our filtering approach to a standard Kalman filter applied to a perturbation-based solution using simulated data ($T = 200$) from the dynamic Taylor Projection solution. Log output is assumed to be observed with measurement error equal to 10% of its standard deviation. As shown in Table 6, TP combined with a time-varying Kalman filter yields substantially lower mean squared errors (MSEs): for TFP z_t, the MSE is less than half that of perturbation; for employment L_t, nearly one-third; and for average unemployed wealth, over 25 times smaller. The final rows show that this gap reflects increasing inaccuracy of the perturbation solution away from steady state: the correlation between z_t^2 and squared filtering error exceeds 0.38 for TFP and 0.60 for unemployed wealth.

Overall, the results in Figures 7, F1, and Table 6 demonstrate that even a simple heterogeneous household model exhibits nonlinearities that are poorly captured by perturbation-based solutions. This suggests that full-information estimation methods relying on such approximations may yield inaccurate results. Our proposed approach offers a more accurate alternative.

Table 6: Mean squared error of filtered state versus true value and correlation between squared error and squared TFP. All MSE's are normalized by the unconditional variance of the relevant state.

Statistic	Method	z_t	m_u^1	m_u^2	m_e^1	m_e^2	L_t
MSE	TP + TV-KF	0.026	0.004	0.018	0.016	0.061	0.008
	KF	0.058	0.111	0.140	0.036	0.067	0.024
MSE ratio	KF/TP + TV-KF	2.3	25.3	7.7	2.3	1.1	2.8
$\text{Corr}(z_t^2, e_t^2)$	TP + TV-KF	0.048	0.039	-0.097	-0.028	-0.139	-0.020
	KF	0.377	0.602	0.545	0.146	0.023	0.408

7 Conclusion

This paper presents a computationally efficient framework for full-information estimation of nonlinear DSGE models by integrating the model solution directly into the filtering step. This eliminates the need for global solution methods and simulation-based filters, enabling accurate estimation of models with rich nonlinearities. We demonstrate the method on two canonical models, achieving estimation speeds of orders of magnitude faster than existing nonlinear approaches. In our main application, we show that labor market frictions generate meaningful state dependence in monetary policy transmission, with impulse response functions and the Phillips Multiplier varying substantially over the cycle. The framework also extends to models with stochastic volatility, regime switching, and heterogeneous agents, offering a general and tractable approach to estimating nonlinear macroeconomic models.

References

Ahn, H. J. and J. D. Hamilton (2022): "Measuring Labor-Force Participation and the Incidence and Duration of Unemployment," *Review of Economic Dynamics*, 44, 1–32.

Andreasen, M. M., J. Fernández-Villaverde, and J. F. Rubio-Ramírez (2018): "The Pruned State-Space System for Non-Linear DSGE Models: Theory and Empirical Applications," *The Review of Economic Studies*, 85, 1–49.

Auclert, A., B. Bardóczy, M. Rognlie, and L. Straub (2021): "Using the Sequence-Space Jacobian to Solve and Estimate Heterogeneous-agent Models," *Econometrica*, 89, 2375–2408.

Barnichon, R. (2010): "Building a Composite Help-Wanted Index," *Economics Letters*, 109, 175–178.

Barnichon, R., D. Debortoli, and C. Matthes (2022): "Understanding the Size of the Government Spending Multiplier: It's in the Sign," *The Review of Economic Studies*, 89, 87–117.

Barnichon, R. and G. Mesters (2021): "The Phillips Multiplier," *Journal of Monetary Economics*, 117, 689–705.

Barro, R. J. (2009): "Rare Disasters, Asset Prices, and Welfare Costs," *American Economic Review*, 99, 243–264.

Bauer, M. D. and E. T. Swanson (2023): "A Reassessment of Monetary Policy Surprises and High-Frequency Identification," *NBER Macroeconomics Annual*, 37, 87–155.

Benigno, P. and G. B. Eggertsson (2023): "It's baaack: The Surge in Inflation in the 2020s and the Return of the Non-Linear Phillips Curve," Tech. rep., National Bureau of Economic Research.

——— (2024): "Slanted-L Phillips Curve," in *AEA Papers and Proceedings*, American Economic Association 2014 Broadway, Suite 305, Nashville, TN 37203, vol. 114, 84–89.

Childers, D., J. Fernández-Villaverde, J. Perla, C. Rackauckas, and P. Wu (2022): "Differentiable State-Space Models and Hamiltonian Monte Carlo Estimation," Tech. rep., National Bureau of Economic Research.

Christiano, L. J., M. Eichenbaum, and M. Trabandt (2016): "Unemployment and Business Cycles," *Econometrica*, 84, 1523–1569.

Cloyne, J., Ò. Jordà, and A. M. Taylor (2023): "State-Dependent Local Projections: Understanding Impulse Response Heterogeneity," Tech. rep., National Bureau of Economic Research.

De Groot, O. (2016): *What Order?: Perturbation Methods for Stochastic Volatility Asset Pricing and Business Cycle Models*.

Den Haan, W. J., M. L. Kobielarz, and P. Rendahl (2015): "Exact Present Solution with Consistent Future Approximation: A Gridless Algorithm to Solve Stochastic Dynamic Models," .

Diamond, P. A. (1982): "Wage Determination and Efficiency in Search Equilibrium," *The Review of Economic Studies*, 49, 217–227.

Dotsey, M., R. G. King, and A. L. Wolman (1999): "State-Dependent Pricing and the General Equilibrium Dynamics of Money and Output," *The Quarterly Journal of Economics*, 114, 655–690.

Durbin, J. and S. J. Koopman (2012): *Time Series Analysis by State Space Methods*, vol. 38, OUP Oxford.

Farmer, L. E. (2021): "The Discretization Filter: A Simple Way to Estimate Nonlinear State Space Models," *Quantitative Economics*, 12, 41–76.

Fernández-Villaverde, J. and O. Levintal (2024): "The Distributional Effects of Asset Returns," Tech. rep., National Bureau of Economic Research.

Fernández-Villaverde, J. and J. F. Rubio-Ramírez (2007): "Estimating Macroeconomic Models: A Likelihood Approach," *The Review of Economic Studies*, 74, 1059–1087.

Friedman, M. and L. Harris (1998): "A Maximum Likelihood Approach for Non-Gaussian Stochastic Volatility Models," *Journal of Business & Economic Statistics*, 16, 284–291.

Gali, J. (2015): *Monetary Policy, Inflation, and the Business Cycle: An Introduction to the New Keynesian Framework and Its Applications*, Princeton University Press, 2 ed.

Galí, J., F. Smets, and R. Wouters (2012): "Unemployment in an Estimated New Keynesian Model," *NBER Macroeconomics Annual*, 26, 329–360.

Gitti, G. (2024): "Nonlinearities in the Regional Phillips Curve with Labor Market Tightness," .

Gonçalves, S., A. M. Herrera, L. Kilian, and E. Pesavento (2023): "State-Dependent Local Projections," .

Gust, C., E. Herbst, D. López-Salido, and M. E. Smith (2017): "The Empirical Implications of the Interest-rate Lower Bound," *American Economic Review*, 107, 1971–2006.

Hamilton, J. D. (1994): *Time Series Analysis*, Princeton University Press.

Herbst, E. and F. Schorfheide (2016): *Bayesian Estimation of DSGE Models*, Princeton University Press.

——— (2019): "Tempered Particle Filtering," *Journal of Econometrics*, 210, 26–44.

Jordà, Ò. (2005): "Estimation and Inference of Impulse Responses by Local Projections," *American Economic Review*, 95, 161–182.

Judd, K. L. (1998): *Numerical Methods in Economics*, MIT press.

Judd, K. L., L. Maliar, and S. Maliar (2017): "Lower Bounds on Approximation Errors to Numerical Solutions of Dynamic Economic Models," *Econometrica*, 85, 991–1012.

Krause, M. U., D. Lopez-Salido, and T. A. Lubik (2008): "Inflation Dynamics with Search Frictions: A Structural Econometric Analysis," *Journal of Monetary Economics*, 55, 892–916.

Krueger, D., K. Mitman, and F. Perri (2016): "Macroeconomics and Household Heterogeneity," in *Handbook of Macroeconomics*, Elsevier, vol. 2, 843–921.

Krusell, P., B. Kuruşçu, and A. A. Smith Jr (2002): "Equilibrium Welfare and Government Policy with Quasi-Geometric Discounting," *Journal of Economic Theory*, 105, 42–72.

Krusell, P. and A. A. Smith, Jr (1998): "Income and Wealth Heterogeneity in the macroeconomy," *Journal of Political Economy*, 106, 867–896.

Levintal, O. (2018): "Taylor Projection: A New Solution Method for Dynamic General Equilibrium Models," *International Economic Review*, 59, 1345–1373.

Liu, L. and M. Plagborg-Møller (2023): "Full-information Estimation of Heterogeneous Agent Models Using Macro and Micro Data," *Quantitative Economics*, 14, 1–35.

Liu, Z., D. F. Waggoner, and T. Zha (2011): "Sources of Macroeconomic Fluctuations: A Regime-Switching DSGE Approach," *Quantitative Economics*, 2, 251–301.

Ljungqvist, L. and T. J. Sargent (2017): "The Fundamental Surplus," *American Economic Review*, 107, 2630–2665.

Mankiw, N. G. (2001): "The Inexorable and Mysterious Tradeoff Between Inflation and Unemployment," *The Economic Journal*, 111, 45–61.

Mennuni, A., J. F. Rubio-Ramírez, and S. Stepanchuk (2024): "Dynamic Perturbation," *The Review of Economic Studies*, advance online publication.

Mortensen, D. T. (1982): "Property Rights and Efficiency in Mating, Racing, and Related Games," *American Economic Review*, 72, 968–979.

Ottonello, P. and T. Winberry (2020): "Financial Heterogeneity and the Investment Channel of Monetary Policy," *Econometrica*, 88, 2473–2502.

Petrosky-Nadeau, N. and L. Zhang (2017): "Solving the Diamond–Mortensen–Pissarides Model Accurately," *Quantitative Economics*, 8, 611–650.

Pissarides, C. A. (1985): "Short-run Equilibrium Dynamics of Unemployment, Vacancies, and Real Wages," *American Economic Review*, 75, 676–690.

Reiter, M. (2009): "Solving Heterogeneous-Agent Models by Projection and Perturbation," *Journal of Economic Dynamics and Control*, 33, 649–665.

Romer, C. D. and D. H. Romer (2004): "A New Measure of Monetary Shocks: Derivation and Implications," *American Economic Review*, 94, 1055–1084.

Schmitt-Grohé, S. and M. Uribe (2004): "Solving Dynamic General Equilibrium Models Using a Second-Order Approximation to the Policy Function," *Journal of Economic Dynamics and Control*, 28, 755–775.

Shimer, R. (2005): "The Cyclical Behavior of Equilibrium Unemployment and Vacancies," *American Economic Review*, 95, 25–49.

Stock, J. H. and M. W. Watson (2020): "Slack and Cyclically Sensitive Inflation," *Journal of Money, Credit and Banking*, 52, 393–428.

Tauchen, G. (1986): "Finite State Markov-Chain Approximations to Univariate and Vector Autoregressions," *Economics Letters*, 20, 177–181.

Tenreyro, S. and G. Thwaites (2016): "Pushing on a String: US Monetary Policy is Less Powerful in Recessions," *American Economic Journal: Macroeconomics*, 8, 43–74.

Thomas, C. (2011): "Search frictions, real rigidities, and inflation dynamics," *Journal of Money, Credit and Banking*, 43, 1131–1164.

Wieland, J. F. and M.-J. Yang (2020): "Financial Dampening," *Journal of Money, Credit and Banking*, 52, 79–113.

Winberry, T. (2018): "A Method for Solving and Estimating Heterogeneous Agent Macro Models," *Quantitative Economics*, 9, 1123–1151.

Winschel, V. and M. Krätzig (2010): "Solving, Estimating, and Selecting Nonlinear Dynamic Models without the Curse of Dimensionality," *Econometrica*, 78, 803–821.

Supplementary Appendix to "Efficient Estimation of Nonlinear DSGE Models"

Eva F. Janssens Sean McCrary

March, 2026

A Smoothing Algorithm

Algorithm 2 Time-Varying Kalman Smoother with Taylor Projections

Initialize: Set $t = T$, $r_T = 0$ and $N_T = 0$.
while $t \geq 1$ **do**
Update Step:

$$r_{t-1} = Z_t' F_t^{-1} v_t + L_t' r_t \tag{A.1}$$

$$N_{t-1} = Z_t' F_t^{-1} Z_t + L_t' N_t L_t \tag{A.2}$$

where $L_t = T_t - K_t Z_t$, and T_t, Z_t, K_t, v_t and F_t were stored from the filter output in Algorithm 1.

Smoothing step:
Compute the smoothed state estimate:

$$\hat{x}_{t|T} = \hat{x}_{t|t-1} + P_{t|t-1} r_{t-1} \tag{A.3}$$

Compute the smoothed covariance:

$$P_{t|T} = P_{t|t-1} - P_{t|t-1} N_{t-1} P_{t|t-1} \tag{A.4}$$

Set back time: Set $t \leftarrow t - 1$ and repeat.
end while

B Data

Table B1: Data details: estimation and filtering

Variable	Details	Transformation	Source
Employment n_t^{obs}, one minus unrate	Percent, Quarterly, Seasonally adjusted	log and Hamilton filtered	UNRATE (FRED)
Market tightness θ_t^{obs}	Vacancies over unrate, Quarterly	log and Hamilton filtered	Barnicon (2010), JTSJOL, UNRATE (FRED)
Nominal rate r_t^{obs}	3-Month Treasury Bill Secondary Market Rate, Discount Basis	Quarterly*, log	DTB3 (FRED)
Inflation $\pi_{1,t}^{obs}$	Gross domestic product (implicit price deflator)	Quarter-to-quarter P_t/P_{t-1}, log	GDPDEF (FRED)
Inflation $\pi_{1,t}^{obs}$	Consumer Price Index (implicit price deflator)	Quarter-to-quarter P_t/P_{t-1}, log	CPIAUCSL (FRED)
Separation rate s_t^{obs}	Implied job-finding rate Shimer (2005)	Quarterly average, log and Hamilton filtered	UEMPLT5, URATE (FRED)

Notes: (*) 3-month treasury bill (R3M) converted to a quarterly interest rate $(100 * ((1 + R3M/100)^{(1/4)} - 1))$.

C Textbook New-Keynesian Model

C.1 Households

There is a infinitely lived representative household that maximizes:

$$\mathbb{E}_0 \left[\sum_{t=0}^{\infty} \beta^t D_t \left\{ \frac{C_t^{1-\tau} - 1}{1-\tau} - \chi \frac{N_t^{1+\eta}}{1+\eta} \right\} \right],$$

where $d_t = \log(D_t)$ is an intertemporal preference shock and follows an AR(1):

$$d_{t+1} = \rho_d d_t + \varepsilon_t^d, \;\; \varepsilon_t^d \sim N(0, \sigma_d^2),$$

subject to a sequence of budget constraints:

$$P_t C_t + B_t = R_{t-1} B_{t-1} + P_t W_t N_t + T_t,$$

where C_t is consumption of the final good, B_t is an uncontingent nominal bond, R_{t-1} is the nominal interest rate, W_t is the real wage, and T_t contains dividends from firms net of taxes and transfers from the government.

The optimal consumptions/saving and labor supply decisions are given by

$$1 = \beta \mathbb{E}_t \left[\frac{D_{t+1}}{D_t} \left(\frac{C_{t+1}}{C_t} \right)^{-\tau} \frac{R_t}{\Pi_{t+1}} \right], \qquad W_t = \frac{\chi N_t^{\eta}}{C_t^{-\tau}},$$

where $\Pi_{t+1} = \frac{P_{t+1}}{P_t}$. The stochastic discount factor is defined as $Q_{t,t+1} = \beta \frac{D_{t+1}}{D_t} \left(\frac{C_{t+1}}{C_t} \right)^{-\tau}$.

C.2 Firms

A competitive final good firm combines a continuum of intermediate goods $j \in [0, 1]$. Intermediate good j is produced by a monopolist with technology $Y_t(j) = Z_t N_t(j)$ where Z_t is an aggregate technology process common to all firms. These firms choose prices $P_t(j)$ and labor inputs $N_t(j)$ to maximize the present discounted value of profit:

$$\mathbb{E}_0 \left[Q_{0,t} \left\{ \frac{P_t(j)}{P_t} Z_t N_t(j) - W_t N_t(j) - \frac{\phi}{2} \left(\frac{P_t(j)}{P_{t-1}(j)} - \Pi \right)^2 Y_t \right\} \right],$$

subject to a sequence of constraints:

$$Z_t N_t(j) = \left(\frac{P_t(j)}{P_t} \right)^{-1/\gamma} Y_t.$$

Optimal choices of $N_t(j)$ and $P_t(j)$ lead to the following optimal price-setting condition:

$$\begin{aligned} 0 = \frac{Z_t N_t(j)}{P_t} - \phi \left(\frac{P_t(j)}{P_{t-1}(j)} - \Pi \right) \frac{Y_t}{P_{t-1,j}} - \frac{1}{\gamma} \left(\frac{P_t(j)}{P_t} - \frac{W_t}{Z_t} \right) \left(\frac{P_t(j)}{P_t} \right)^{-1/\gamma - 1} \frac{Y_t}{P_t} \\ + \phi \mathbb{E}_t \left[Q_{t,t+1} \left(\frac{P_{t+1}(j)}{P_t(j)} - \Pi \right) \frac{P_{t+1}(j)}{P_t(j)^2} Y_{t+1} \right]. \end{aligned}$$

In a symmetric equilibrium $P_t(j) = P_t$ and $Y_t(j) = Z_t N_t(j) = Z_t N_t$ for all j, so this simplifies to:

$$\frac{1}{\gamma}\left(1 - \frac{W_t}{Z_t}\right) = 1 - \phi\left(\Pi_t - \Pi\right)\Pi_t + \phi\mathbb{E}_t\left[Q_{t,t+1}\left(\Pi_{t+1} - \Pi\right)\Pi_{t+1}\frac{Y_{t+1}}{Y_t}\right].$$

C.3 Government

The government levies lump-sum taxes and runs a balanced budget. The monetary authority follows a Taylor type rule:

$$\frac{R_t}{R} = \left(\frac{\Pi_t}{\Pi}\right)^{\phi_\pi}\left(\frac{Y_t}{Y}\right)^{\phi_y} e^{m_t},$$

where m_t is an exogenous monetary policy shock that follows an AR(1):

$$m_{t+1} = \rho_m m_t + \varepsilon_t^m, \quad \varepsilon_t^m \sim N(0, \sigma_m^2).$$

C.4 Steady State

We focus on a non-stochastic steady state with inflation Π equal to the monetary authority target which implies $R = \Pi/\beta$, and the parameter χ normalizes steady state output Y (which equals N) to be unity: $\chi = 1 - \gamma$. Note, the first-order condition for labor supply implies $W = \chi$, so γ is the steady state wage markdown.

C.5 Equilibrium

The equilibrium conditions for market clearing in the labor and goods markets are:

$$Y_t = C_t = N_t Z_t, \qquad W_t = (1-\gamma)N_t^\eta C_t^\tau = (1-\gamma)N_t^{\eta+\tau}Z_t^\tau.$$

A minimal state representation consists of states $x_t = (z_t, d_t, m_t)$ and policies $\{\Pi(x_t), N(x_t)\}$ defined through the equilibrium conditions (substituting market clearing conditions where appropriate). Using the steady state relations and letting lower case letters denote log-deviations from steady state values e.g. $n_t =$

$\ln N_t - \ln N$, the equilibrium conditions become:[1]

$$\begin{aligned}
\text{Euler/IS}: \; 1 &= \mathbb{E}_t\left[e^{(\rho_d-1)d_t+\varepsilon^d_{t+1}-\tau\left(n_{t+1}-n_t+(\rho_z-1)z_t+\varepsilon^z_{t+1}\right)+r_t-\pi_{t+1}}\right] \\
\text{NK-Phillips}: \; \kappa\left(1-e^{(\eta+\tau)n_t+(\tau-1)z}\right) &= -\left(e^{\pi_t}-1\right)e^{\pi_t} \\
&\quad + \beta\mathbb{E}_t\left[e^{(\rho_d-1)d_t+\varepsilon^d_{t+1}+(1-\tau)\left(n_{t+1}-n_t+(\rho_z-1)z_t+\varepsilon^z_{t+1}\right)}\left(e^{\pi_{t+1}}-1\right)e^{\pi_{t+1}}\right] \\
\text{Taylor Rule}: \; r_t &= \phi_\pi\pi_t + \phi_y(n_t+z_t) + m_t.
\end{aligned}$$

C.6 Local Approximation

The first step is to assume the policies are linear in logs:

$$\begin{aligned}
\pi_t &= a_0 + a_1 z_t + a_2 d_t + a_3 m_t \\
n_t &= b_0 + b_1 z_t + b_2 d_t + b_3 m_t.
\end{aligned}$$

This implies the future policies are of the form:

$$\begin{aligned}
\pi_{t+1} &= a_0 + a_1\rho_z z_t + a_1\varepsilon^z_{t+1} + a_2\rho_d d_t + a_2\varepsilon^d_{t+1} + a_3\rho_m m_t + a_3\varepsilon^m_{t+1} \\
n_{t+1} &= b_0 + b_1\rho_z z_t + b_1\varepsilon^z_{t+1} + b_2\rho_d d_t + b_2\varepsilon^d_{t+1} + b_3\rho_m m_t + b_3\varepsilon^m_{t+1}.
\end{aligned}$$

Moreover, it implies:

$$n_{t+1} - n_t = b_1(\rho_z-1)z_t + b_1\varepsilon^z_{t+1} + b_2(\rho_d-1)d_t + b_2\varepsilon^d_{t+1} + b_3(\rho_m-1)m_t + b_3\varepsilon^m_{t+1}.$$

The goal of the local approximation method is to solve for the policy coefficients $\boldsymbol{a}$ and $\boldsymbol{b}$ at a given state $x_t = (z_t, d_t, m_t)$.

Euler equation Consider the Euler equation with the policies substituted:

$$\begin{aligned}
1 =& e^{(\rho_d-1)d_t-\tau\left[b_1(\rho_z-1)z_t+b_2(\rho_d-1)d_t+b_3(\rho_m-1)m_t\right]-\tau(\rho_z-1)z_t+r_t-a_1-a_1\rho_z z_t-a_2\rho_d d_t-a_3\rho_m m_t} \\
&\cdot \mathbb{E}_t\left[e^{\varepsilon^d_{t+1}-\tau(b_1\varepsilon^z_{t+1}+b_2\varepsilon^d_{t+1}+b_3\varepsilon^m_{t+1})-\tau\varepsilon^z_{t+1}-a_1\varepsilon^z_{t+1}-a_2\varepsilon^d_{t+1}-a_3\varepsilon^m_{t+1}}\right].
\end{aligned}$$

[1] We define $\kappa = \frac{1-\gamma}{\phi\Pi^2\gamma}$.

Collecting terms in the expectation yields:

$$\mathbb{E}_t\left[e^{\varepsilon^d_{t+1}-\tau(b_1\varepsilon^z_{t+1}+b_2\varepsilon^d_{t+1}+b_3\varepsilon^m_{t+1})-\tau\varepsilon^z_{t+1}-a_1\varepsilon^z_{t+1}-a_2\varepsilon^d_{t+1}-a_3\varepsilon^m_{t+1}}\right]=\mathbb{E}_t\left[e^{(1-\tau b_2-a_2)\varepsilon^d_{t+1}-(\tau(b_1+1)+a_1)\varepsilon^z_{t+1}-\tau(b_3+a_3)\varepsilon^m_{t+1}}\right].$$

For a mean zero normal random variable X, and constant c, the expectation satisfies:

$$\mathbb{E}\left[e^{cX}\right]=e^{\frac{1}{2}c^2\sigma_x^2},$$

so the Euler equation simplifies to:

$$\begin{aligned}1=&\exp\left\{(\rho_d-1)d_t-\tau\left[b_1(\rho_z-1)z_t+b_2(\rho_d-1)d_t+b_3(\rho_m-1)m_t\right]-\tau(\rho_z-1)z_t+r_t-a_1-a_1\rho_z z_t-a_2\rho_d d_t-a_3\rho_m m_t\right\}\\&\cdot\exp\left\{\frac{1}{2}\left\{(1-\tau b_2-a_2)^2\sigma_d^2+(\tau(b_1+1)+a_1)^2\sigma_z^2+\tau^2(b_3+a_3)^2\sigma_m^2\right\}\right\}.\end{aligned}$$

Note, by taking logs and substituting the Taylor Rule, this is equivalent to:

$$\begin{aligned}0=&(\rho_d-1)d_t+\tau\left[b_1(1-\rho_z)z_t+b_2(1-\rho_d)d_t+b_3(1-\rho_m)m_t\right]+\tau(1-\rho_z)z_t\\&+\phi_\pi(a_0+a_1z_t+a_2d_t+a_3m_t)+\phi_y(b_0+b_1z_t+b_2d_t+b_3m_t+z_t)+m_t\\&-(a_0+a_1\rho_z z_t+a_2\rho_d d_t+a_3\rho_m m_t)\\&+\frac{1}{2}\left\{(1-\tau b_2-a_2)^2\sigma_d^2+(\tau(b_1+1)+a_1)^2\sigma_z^2+\tau^2(b_3+a_3)^2\sigma_m^2\right\},\end{aligned}$$

which implies the variance terms show up in the Euler equation, but not the partial derivatives of the Euler equation with respect to the states, leading to a sparse Jacobian.

Pricing equation Now consider the pricing equation with the policies substituted:

$$\begin{aligned}&\frac{1-\gamma}{\Pi^2\phi\gamma}\left(1-e^{(\eta+\tau)(b_0+b_1z_t+b_2d_t+b_3m_t)+(\tau-1)z_t}\right)=-e^{2(a_0+a_1z_t+a_2d_t+a_3m_t)}+e^{a_0+a_1z_t+a_2d_t+a_3m_t}\\&+\beta e^{(\rho_d-1)d_t+(1-\tau)\left\{b_1(\rho_z-1)z_t+b_2(\rho_d-1)d_t+b_3(\rho_m-1)m_t+(\rho_z-1)z_t\right\}+2(a_0+a_1\rho_z z_t+a_2\rho_d d_t+a_3\rho_m m_t)}\\&\cdot\mathbb{E}_t\left[e^{\varepsilon^d_{t+1}+(1-\tau)\left\{b_1\varepsilon^z_{t+1}+b_2\varepsilon^d_{t+1}+b_3\varepsilon^m_{t+1}+\varepsilon^z_{t+1}\right\}+2(a_1\varepsilon^z_{t+1}+a_2\varepsilon^d_{t+1}+a_3\varepsilon^m_{t+1})}\right]\\&-\beta e^{(\rho_d-1)d_t+(1-\tau)\left\{b_1(\rho_z-1)z_t+b_2(\rho_d-1)d_t+b_3(\rho_m-1)m_t+(\rho_z-1)z_t\right\}+a_0+a_1\rho_z z_t+a_2\rho_d d_t+a_3\rho_m m_t}\\&\cdot\mathbb{E}_t\left[e^{\varepsilon^d_{t+1}+(1-\tau)\left\{b_1\varepsilon^z_{t+1}+b_2\varepsilon^d_{t+1}+b_3\varepsilon^m_{t+1}+\varepsilon^z_{t+1}\right\}+a_1\varepsilon^z_{t+1}+a_2\varepsilon^d_{t+1}+a_3\varepsilon^m_{t+1}}\right].\end{aligned}$$

Focusing on the expectation terms, we have the following:

$$\begin{aligned}
&\mathbb{E}_t\left[e^{\varepsilon^d_{t+1}+(1-\tau)\left\{b_1\varepsilon^z_{t+1}+b_2\varepsilon^d_{t+1}+b_3\varepsilon^m_{t+1}+\varepsilon^z_{t+1}\right\}+2(a_1\varepsilon^z_{t+1}+a_2\varepsilon^d_{t+1}+a_3\varepsilon^m_{t+1})}\right] \\
&= e^{\frac{1}{2}\left\{(1+(1-\tau)b_2+2a_2)^2\sigma_d^2+((1-\tau)(b_1+1)+2a_1)^2\sigma_z^2+((1-\tau)b_3+2a_3)^2\sigma_m^2\right\}}, \\
&\mathbb{E}_t\left[e^{\varepsilon^d_{t+1}+(1-\tau)\left\{b_1\varepsilon^z_{t+1}+b_2\varepsilon^d_{t+1}+b_3\varepsilon^m_{t+1}+\varepsilon^z_{t+1}\right\}+a_1\varepsilon^z_{t+1}+a_2\varepsilon^d_{t+1}+a_3\varepsilon^m_{t+1}}\right] \\
&= e^{\frac{1}{2}\left\{(1+(1-\tau)b_2+a_2)^2\sigma_d^2+((1-\tau)(b_1+1)+a_1)^2\sigma_z^2+((1-\tau)b_3+a_3)^2\sigma_m^2\right\}},
\end{aligned}$$

which implies the pricing equation simplifies to:

$$\begin{aligned}
&\kappa\left(1-e^{(\eta+\tau)(b_0+b_1z_t+b_2d_t+b_3m_t)+(\tau-1)z_t}\right) = -e^{2(a_0+a_1z_t+a_2d_t+a_3m_t)}+e^{a_0+a_1z_t+a_2d_t+a_3m_t} \\
&+\beta e^{(\rho_d-1)d_t+(1-\tau)\left\{b_1(\rho_z-1)z_t+b_2(\rho_d-1)d_t+b_3(\rho_m-1)m_t+(\rho_z-1)z_t\right\}+2(a_0+a_1\rho_zz_t+a_2\rho_dd_t+a_3\rho_mm_t)} \\
&\cdot e^{\frac{1}{2}\left\{(1+(1-\tau)b_2+2a_2)^2\sigma_d^2+((1-\tau)(b_1+1)+2a_1)^2\sigma_z^2+((1-\tau)b_3+2a_3)^2\sigma_m^2\right\}} \\
&-\beta e^{(\rho_d-1)d_t+(1-\tau)\left\{b_1(\rho_z-1)z_t+b_2(\rho_d-1)d_t+b_3(\rho_m-1)m_t+(\rho_z-1)z_t\right\}+a_0+a_1\rho_zz_t+a_2\rho_dd_t+a_3\rho_mm_t} \\
&\cdot e^{\frac{1}{2}\left\{(1+(1-\tau)b_2+a_2)^2\sigma_d^2+((1-\tau)(b_1+1)+a_1)^2\sigma_z^2+((1-\tau)b_3+a_3)^2\sigma_m^2\right\}},
\end{aligned}$$

where $\kappa = \frac{1-\gamma}{\Pi^2\phi\gamma}$. Here, the derivatives of the residual function and elements of the Jacobian are more elaborate, but given that this is an analytic expression we can rely on symbolic differentiation to obtain the results.

D NK-DMP Model

Here we describe the additional details of the NK-DMP model. Collecting the equilibrium conditions together we have:

$$\begin{aligned}
1 &= \beta\mathbb{E}_t\left[\frac{D_{t+1}}{D_t}\left(\frac{N_{t+1}Z_{t+1}}{N_tZ_t}\right)^{-\tau}\frac{R_t}{\Pi_{t+1}}\right] \\
\frac{\Omega_t}{\gamma} &= 1-\phi\left(\Pi_t-\Pi\right)\Pi_t+\phi\beta\mathbb{E}_t\left[\frac{D_{t+1}}{D_t}\left(\frac{N_{t+1}Z_{t+1}}{N_tZ_t}\right)^{1-\tau}\left(\Pi_{t+1}-\Pi\right)\Pi_{t+1}\right] \\
\frac{c}{Q_t} &= (1-\eta)\left((1-\Omega_t)e^{z_t}-\nu\right)+\beta\mathbb{E}_t\left[(1-\delta_{t+1})\frac{D_{t+1}}{D_t}\left(\frac{N_{t+1}Z_{t+1}}{N_tZ_t}\right)^{-\tau}\frac{c}{Q_{t+1}}\right]
\end{aligned}$$

with auxiliary equations

$$
\begin{aligned}
\frac{R_t}{R} &= \left(\frac{\Pi_t}{\Pi}\right)^{\phi_\pi} \left(\frac{N_t Z_t}{N}\right)^{\phi_y} e^{m_t} \\
N_t &= (1-\delta_t)N_{t-1} + Q_t \Theta_t \left(1-(1-\delta_t)N_{t-1}\right) \\
Q_t &= A_t \Theta_t^{-\alpha}, \qquad \delta_t = \delta e^{s_t}, \qquad A_t = A e^{a_t} \\
z_t &= \rho_z z_{t-1} + \varepsilon_t^z, \quad d_t = \rho_d d_{t-1} + \varepsilon_t^d, \quad m_t = \rho_m m_{t-1} + \varepsilon_t^m, \\
s_t &= \rho_s s_{t-1} + \varepsilon_t^s, \quad a_t = \rho_a a_{t-1} + \varepsilon_t^a
\end{aligned}
$$

where $z_t = \ln Z_t$ and $d_t = \ln D_t$. A minimal state representation has six states $x_t = (N_{t-1}, z_t, d_t, m_t, s_t, a_t)$ and three policies $\{\theta(x_t), \Pi(x_t), \omega(x_t)\}$.

D.1 Steady State

We focus on a non-stochastic steady state where inflation is at the monetary authority target Π. This implies $\beta = \Pi/R$ and $\omega = \gamma$. In the labor market, we normalize $\theta = 1$, and $q = 0.7$, and $N = 0.945$. This implies $A = 0.7$ and $\delta \approx 0.1358$.[2]

D.2 Local Approximation

In what follows it will be useful to write variables in terms of log deviations from their steady state values, e.g., $n_t = \ln N_t - \ln N$. This yields an equilibrium system:

$$
\begin{aligned}
1 &= \mathbb{E}_t\left[e^{d_{t+1}-d_t-\tau(n_{t+1}+z_{t+1}-n_t-z_t)+r_t-\pi_{t+1}}\right] \\
\frac{1}{\phi\Pi^2}\left(e^{\omega_t}-1\right) &= -\left(e^{\pi_t}-1\right)e^{\pi_t} + \beta\mathbb{E}_t\left[e^{d_{t+1}-d_t+(1-\tau)(n_{t+1}+z_{t+1}-n_t-z_t)}\left(e^{\pi_{t+1}}-1\right)e^{\pi_{t+1}}\right] \\
e^{-q_t} &= \frac{Q(1-\eta)}{c}\left((1-\gamma e^{\omega_t})e^{z_t}-\nu\right) + \beta\mathbb{E}_t\left[(1-\delta e^{s_{t+1}})e^{d_{t+1}-d_t-\tau(n_{t+1}+z_{t+1}-n_t-z_t)-q_{t+1}}\right] \\
e^{n_t-n_{t-1}} &= (1-\delta e^{s_t}) + Q\theta e^{q_t+\theta_t}\left(\frac{1}{N}e^{-n_{t-1}} - (1-\delta e^{s_t})\right),
\end{aligned}
$$

[2]The value of δ is implied by the law of motion for employment $\delta N = q\theta - q\theta(1-\delta)N \Rightarrow \delta = \frac{1-N}{N}\frac{q\theta}{1-q\theta} \approx 0.1358$

where

$$\begin{aligned}
\theta_t &= b_{10} + b_{11} n_{t-1} + b_{12} z_t + b_{13} d_t + b_{14} m_t + b_{15} s_t + b_{16} a_t \\
\pi_t &= b_{20} + b_{21} n_{t-1} + b_{22} z_t + b_{23} d_t + b_{24} m_t + b_{25} s_t + b_{26} a_t \\
\omega_t &= b_{30} + b_{31} n_{t-1} + b_{32} z_t + b_{33} d_t + b_{34} m_t + b_{35} s_t + b_{36} a_t \\
n_t &= b_{40} + b_{41} n_{t-1} + b_{42} z_t + b_{43} d_t + b_{44} m_t + b_{45} s_t + b_{46} a_t \\
q_t &= a_t - \alpha \theta_t \\
r_t &= \phi_\pi \pi_t + \phi_y (n_t + z_t) + m_t .
\end{aligned}$$

This implies:

$$\begin{aligned}
n_{t+1} - n_t &= b_{41}(n_t - n_{t-1}) + b_{42}(z_{t+1} - z_t) + b_{43}(d_{t+1} - d_t) + b_{44}(m_{t+1} - m_t) + b_{45}(s_{t+1} - s_t) + b_{46}(a_{t+1} - a_t) \\
&= b_{41} b_{40} + b_{41}(b_{41} - 1) n_{t-1} + b_{42}(\rho_z - 1 + b_{41}) z_t + b_{43}(\rho_d - 1 + b_{41}) d_t + b_{44}(\rho_m - 1 + b_{41}) m_t \\
&\quad + b_{45}(\rho_s - 1 + b_{41}) s_t + b_{46}(\rho_a - 1 + b_{41}) a_t + b_{42} \varepsilon^z_{t+1} + b_{43} \varepsilon^d_{t+1} + b_{44} \varepsilon^m_{t+1} + b_{45} \varepsilon^s_{t+1} + b_{46} \varepsilon^a_{t+1}
\end{aligned}$$

The change in employment, $n_{t+1} - n_t$, consists of a deterministic component known at time t and a stochastic innovation realized at $t+1$, and can be written as:

$$n_{t+1} - n_t = B^n_0 + B^n_1 x_t + B^n_2 \varepsilon_{t+1}.$$

Similarly, π_{t+1} and the exogenous shocks can be written as:

$$\begin{aligned}
\pi_{t+1} &= b_{20} + b_{21} n_t + b_{22} z_{t+1} + b_{23} d_{t+1} + b_{24} m_{t+1} + b_{25} s_{t+1} + b_{26} a_{t+1} \\
&= b_{20} + b_{21}(b_{40} + b_{41} n_{t-1} + b_{42} z_t + b_{43} d_t + b_{44} m_t + b_{45} s_t + b_{46} a_t) \\
&\quad + b_{22} \rho_z z_t + b_{23} \rho_d d_t + b_{24} \rho_m m_t + b_{25} \rho_s s_t + b_{26} \rho_a a_t \\
&\quad + b_{22} \varepsilon^z_{t+1} + b_{23} \varepsilon^d_{t+1} + b_{24} \varepsilon^m_{t+1} + b_{25} \varepsilon^s_{t+1} + b_{26} \varepsilon^a_{t+1} \\
&= B^\pi_0 + B^\pi_1 x_t + B^\pi_2 \varepsilon_{t+1} \\
z_{t+1} - z_t &= (\rho_z - 1) z_t + \varepsilon^z_{t+1} \\
d_{t+1} - d_t &= (\rho_d - 1) d_t + \varepsilon^d_{t+1}.
\end{aligned}$$

Finally, θ_{t+1} and q_{t+1} can be written as:

$$\begin{aligned}
\theta_{t+1} &= b_{10} + b_{11}n_t + b_{12}z_{t+1} + b_{13}d_{t+1} + b_{14}m_{t+1} + b_{15}s_{t+1} + b_{16}a_{t+1} \\
&= b_{10} + b_{11}(b_{40} + b_{41}n_{t-1} + b_{42}z_t + b_{43}d_t + b_{44}m_t + b_{45}s_t + b_{46}a_t) \\
&\quad + b_{12}\rho_z z_t + b_{13}\rho_d d_t + b_{14}\rho_m m_t + b_{15}\rho_s s_t + b_{16}\rho_a a_t \\
&\quad + b_{12}\varepsilon^z_{t+1} + b_{13}\varepsilon^d_{t+1} + b_{14}\varepsilon^m_{t+1} + b_{15}\varepsilon^s_{t+1} + b_{16}\varepsilon^a_{t+1} \\
&= B^\theta_0 + B^\theta_1 x_t + B^\theta_2 \varepsilon_{t+1} \\
q_{t+1} &= \rho_a a_t + \varepsilon^a_{t+1} - \alpha B^\theta_0 - \alpha B^\theta_1 x_t - \alpha B^\theta_2 \varepsilon_{t+1}.
\end{aligned}$$

Euler Equation Consider the Euler equation:

$$1 = \mathbb{E}_t \left[e^{d_{t+1} - d_t - \tau(n_{t+1} + z_{t+1} - n_t - z_t) + r_t - \pi_{t+1}} \right].$$

Using the previous expressions, we can write the Euler equation compactly as:

$$1 = e^{(\rho_d - 1)d_t - \tau(\rho_z - 1)z_t - \tau B^n_0 - \tau B^n_1 x_t + r_t - B^\pi_0 - B^\pi_1 x_t} \mathbb{E}_t \left[e^{\varepsilon^d_{t+1} - \tau B^n_2 \varepsilon_{t+1} - \tau \varepsilon^z_{t+1} - B^\pi_2 \varepsilon_{t+1}} \right],$$

and the expectation can be expressed in closed form as:

$$\begin{aligned}
&\mathbb{E}_t \left[e^{\varepsilon^d_{t+1} - \tau B^n_2 \varepsilon_{t+1} - \tau \varepsilon^z_{t+1} - B^\pi_2 \varepsilon_{t+1}} \right] \\
&= \mathbb{E}_t \left[e^{\varepsilon^d_{t+1} - \tau(b_{42}\varepsilon^z_{t+1} + b_{43}\varepsilon^d_{t+1} + b_{44}\varepsilon^m_{t+1} + b_{45}\varepsilon^s_{t+1} + b_{46}\varepsilon^a_{t+1}) - \tau\varepsilon^z_{t+1} - (b_{22}\varepsilon^z_{t+1} + b_{23}\varepsilon^d_{t+1} + b_{24}\varepsilon^m_{t+1} + b_{25}\varepsilon^s_{t+1} + b_{26}\varepsilon^a_{t+1})} \right] \\
&= \mathbb{E}_t \left[e^{(1 - \tau b_{43} - b_{23})\varepsilon^d_{t+1} - (\tau(b_{42}+1) + b_{22})\varepsilon^z_{t+1} - (\tau b_{44} + b_{24})\varepsilon^m_{t+1} - (\tau b_{45} + b_{25})\varepsilon^s_{t+1} - (\tau b_{46} + b_{26})\varepsilon^a_{t+1}} \right] \\
&= e^{\frac{1}{2}\left((1 - \tau b_{43} - b_{23})^2\sigma^2_d + (\tau(b_{42}+1) + b_{22})^2\sigma^2_z + (\tau b_{44} + b_{24})^2\sigma^2_m + (\tau b_{45} + b_{25})^2\sigma^2_s + (\tau b_{46} + b_{26})^2\sigma^2_a\right)}.
\end{aligned}$$

Pricing equation Consider the optimal price-setting condition:

$$\frac{1}{\phi \Pi^2}\left(e^{\omega_t} - 1\right) = -\left(e^{\pi_t} - 1\right)e^{\pi_t} + \beta \mathbb{E}_t \left[e^{d_{t+1} - d_t + (1-\tau)(n_{t+1} + z_{t+1} - n_t - z_t)} \left(e^{\pi_{t+1}} - 1\right) e^{\pi_{t+1}} \right].$$

The continuation value can be solved in closed form given the linear policies, first note:

$$\begin{aligned}
&\mathbb{E}_t\left[e^{d_{t+1}-d_t+(1-\tau)(n_{t+1}+z_{t+1}-n_t-z_t)}\left(e^{\pi_{t+1}}-1\right)e^{\pi_{t+1}}\right]\\
&=\mathbb{E}_t\left[e^{d_{t+1}-d_t+(1-\tau)(n_{t+1}+z_{t+1}-n_t-z_t)}\left(e^{2\pi_{t+1}}-e^{\pi_{t+1}}\right)\right]\\
&=e^{(\rho_d-1)d_t+(1-\tau)\left[(\rho_z-1)z_t+B_0^n+B_1^n x_t\right]}\mathbb{E}_t\left[e^{\varepsilon^d_{t+1}+(1-\tau)(B_2^n\varepsilon_{t+1}+\varepsilon^z_{t+1})}\left(e^{2\pi_{t+1}}-e^{\pi_{t+1}}\right)\right],
\end{aligned}$$

and the remaining expectation term can be written as:

$$\mathbb{E}_t\left[e^{\varepsilon^d_{t+1}+(1-\tau)(B_2^n\varepsilon_{t+1}+\varepsilon^z_{t+1})+2\pi_{t+1}}\right]-\mathbb{E}_t\left[e^{\varepsilon^d_{t+1}+(1-\tau)(B_2^n\varepsilon_{t+1}+\varepsilon^z_{t+1})+\pi_{t+1}}\right],$$

where

$$\begin{aligned}
\mathbb{E}_t\left[e^{\varepsilon^d_{t+1}+(1-\tau)(B_2^n\varepsilon_{t+1}+\varepsilon^z_{t+1})+2\pi_{t+1}}\right]&=e^{2B_0^\pi+2B_1^\pi x_t}\mathbb{E}_t\left[e^{\varepsilon^d_{t+1}+(1-\tau)(B_2^n\varepsilon_{t+1}+\varepsilon^z_{t+1})+2B_2^\pi\varepsilon_{t+1}}\right]\\
\mathbb{E}_t\left[e^{\varepsilon^d_{t+1}+(1-\tau)(B_2^n\varepsilon_{t+1}+\varepsilon^z_{t+1})+\pi_{t+1}}\right]&=e^{B_0^\pi+B_1^\pi x_t}\mathbb{E}_t\left[e^{\varepsilon^d_{t+1}+(1-\tau)(B_2^n\varepsilon_{t+1}+\varepsilon^z_{t+1})+B_2^\pi\varepsilon_{t+1}}\right].
\end{aligned}$$

Expanding the expectation terms and solving yields:

$$\begin{aligned}
&\mathbb{E}_t\left[e^{\varepsilon^d_{t+1}+(1-\tau)(B_2^n\varepsilon_{t+1}+\varepsilon^z_{t+1})+2B_2^\pi\varepsilon_{t+1}}\right]\\
&=\mathbb{E}_t\left[e^{\varepsilon^d_{t+1}+(1-\tau)(b_{42}\varepsilon^z_{t+1}+b_{43}\varepsilon^d_{t+1}+b_{44}\varepsilon^m_{t+1}+b_{45}\varepsilon^s_{t+1}+b_{46}\varepsilon^a_{t+1}+\varepsilon^z_{t+1})+2\left(b_{22}\varepsilon^z_{t+1}+b_{23}\varepsilon^d_{t+1}+b_{24}\varepsilon^m_{t+1}+b_{25}\varepsilon^s_{t+1}+b_{26}\varepsilon^a_{t+1}\right)}\right]\\
&=\mathbb{E}_t\left[e^{(1+(1-\tau)b_{43}+2b_{23})\varepsilon^d_{t+1}+((1-\tau)(b_{42}+1)+2b_{22})\varepsilon^z_{t+1}+((1-\tau)b_{44}+2b_{24})\varepsilon^m_{t+1}+((1-\tau)b_{45}+2b_{25})\varepsilon^s_{t+1}+((1-\tau)b_{46}+2b_{26})\varepsilon^a_{t+1}}\right]\\
&=e^{\frac{1}{2}\left((1+(1-\tau)b_{43}+2b_{23})^2\sigma_d^2+((1-\tau)(b_{42}+1)+2b_{22})^2\sigma_z^2+((1-\tau)b_{44}+2b_{24})^2\sigma_m^2+((1-\tau)b_{45}+2b_{25})^2\sigma_s^2+((1-\tau)b_{46}+2b_{26})^2\sigma_a^2\right)}
\end{aligned}$$

$$\begin{aligned}
&\mathbb{E}_t\left[e^{\varepsilon^d_{t+1}+(1-\tau)(B_2^n\varepsilon_{t+1}+\varepsilon^z_{t+1})+B_2^\pi\varepsilon_{t+1}}\right]\\
&=\mathbb{E}_t\left[e^{\varepsilon^d_{t+1}+(1-\tau)(b_{42}\varepsilon^z_{t+1}+b_{43}\varepsilon^d_{t+1}+b_{44}\varepsilon^m_{t+1}+b_{45}\varepsilon^s_{t+1}+b_{46}\varepsilon^a_{t+1}+\varepsilon^z_{t+1})+b_{22}\varepsilon^z_{t+1}+b_{23}\varepsilon^d_{t+1}+b_{24}\varepsilon^m_{t+1}+b_{25}\varepsilon^s_{t+1}+b_{26}\varepsilon^a_{t+1}}\right]\\
&=\mathbb{E}_t\left[e^{(1+(1-\tau)b_{43}+b_{23})\varepsilon^d_{t+1}+((1-\tau)(b_{42}+1)+b_{22})\varepsilon^z_{t+1}+((1-\tau)b_{44}+b_{24})\varepsilon^m_{t+1}+((1-\tau)b_{45}+b_{25})\varepsilon^s_{t+1}+((1-\tau)b_{46}+b_{26})\varepsilon^a_{t+1}}\right]\\
&=e^{\frac{1}{2}\left((1+(1-\tau)b_{43}+b_{23})^2\sigma_d^2+((1-\tau)(b_{42}+1)+b_{22})^2\sigma_z^2+((1-\tau)b_{44}+b_{24})^2\sigma_m^2+((1-\tau)b_{45}+b_{25})^2\sigma_s^2+((1-\tau)b_{46}+b_{26})^2\sigma_a^2\right)}.
\end{aligned}$$

Job creation condition Consider the job creation condition:

$$e^{-q_t}=\frac{Q(1-\eta)}{c}\left((1-\gamma e^{\omega_t})e^{z_t}-\nu\right)+\beta\mathbb{E}_t\left[(1-\delta e^{s_{t+1}})e^{d_{t+1}-d_t-\tau(n_{t+1}+z_{t+1}-n_t-z_t)-q_{t+1}}\right].$$

The continuation value can be solved in closed form given the linear policies, note:

$$\begin{aligned}
&\mathbb{E}_t\left[(1-\delta e^{s_{t+1}})e^{d_{t+1}-d_t-\tau(n_{t+1}+z_{t+1}-n_t-z_t)-q_{t+1}}\right] \\
&= \mathbb{E}_t\left[(1-\delta e^{s_{t+1}})e^{d_{t+1}-d_t-\tau\left(B_0^n+B_1^n x_t+B_2^n\varepsilon_{t+1}+z_{t+1}-z_t\right)-\rho_a a_t-\varepsilon^a_{t+1}+\alpha B_0^\theta+\alpha B_1^\theta x_t+\alpha B_2^\theta\varepsilon_{t+1}}\right] \\
&= e^{(\rho_d-1)d_t-\tau(\rho_z-1)z_t-\tau B_0^n-\tau B_1^n x_t-\rho_a a_t+\alpha B_0^\theta+\alpha B_1^\theta x_t}\mathbb{E}_t\left[(1-\delta e^{s_{t+1}})e^{\varepsilon^d_{t+1}-\tau\left(B_2^n\varepsilon_{t+1}+\varepsilon^z_{t+1}\right)-\varepsilon^a_{t+1}+\alpha B_2^\theta\varepsilon_{t+1}}\right]
\end{aligned}$$

The remaining expectation term can be written as:

$$\begin{aligned}
&\mathbb{E}_t\left[(1-\delta e^{s_{t+1}})e^{\varepsilon^d_{t+1}-\tau\left(B_2^n\varepsilon_{t+1}+\varepsilon^z_{t+1}\right)-\varepsilon^a_{t+1}+\alpha B_2^\theta\varepsilon_{t+1}}\right] \\
&= \mathbb{E}_t\left[e^{\varepsilon^d_{t+1}-\tau\left(B_2^n\varepsilon_{t+1}+\varepsilon^z_{t+1}\right)-\varepsilon^a_{t+1}+\alpha B_2^\theta\varepsilon_{t+1}}\right] \\
&- \delta e^{\rho_s s_t}\mathbb{E}_t\left[e^{\varepsilon^s_{t+1}+\varepsilon^d_{t+1}-\tau\left(B_2^n\varepsilon_{t+1}+\varepsilon^z_{t+1}\right)-\varepsilon^a_{t+1}+\alpha B_2^\theta\varepsilon_{t+1}}\right],
\end{aligned}$$

where

$$\begin{aligned}
&\mathbb{E}_t\left[e^{\varepsilon^d_{t+1}-\tau\left(B_2^n\varepsilon_{t+1}+\varepsilon^z_{t+1}\right)-\varepsilon^a_{t+1}+\alpha B_2^\theta\varepsilon_{t+1}}\right] \\
&= \mathbb{E}_t\left[e^{\varepsilon^d_{t+1}-\tau\left(b_{42}\varepsilon^z_{t+1}+b_{43}\varepsilon^d_{t+1}+b_{44}\varepsilon^m_{t+1}+b_{45}\varepsilon^s_{t+1}+b_{46}\varepsilon^a_{t+1}+\varepsilon^z_{t+1}\right)-\varepsilon^a_{t+1}+\alpha\left(b_{12}\varepsilon^z_{t+1}+b_{13}\varepsilon^d_{t+1}+b_{14}\varepsilon^m_{t+1}+b_{15}\varepsilon^s_{t+1}+b_{16}\varepsilon^a_{t+1}\right)}\right] \\
&= e^{\frac{1}{2}\left((\alpha b_{13}-\tau b_{43}+1)^2\sigma_d^2+(\alpha b_{12}-\tau b_{42})^2\sigma_z^2+(\alpha b_{14}-\tau b_{44})^2\sigma_m^2+(\alpha b_{15}-\tau b_{45})^2\sigma_s^2+(\alpha b_{16}-\tau b_{46}-1)^2\sigma_a^2\right)} \\
&\mathbb{E}_t\left[e^{\varepsilon^s_{t+1}+\varepsilon^d_{t+1}-\tau\left(B_2^n\varepsilon_{t+1}+\varepsilon^z_{t+1}\right)-\varepsilon^a_{t+1}+\alpha B_2^\theta\varepsilon_{t+1}}\right] \\
&= \mathbb{E}_t\left[e^{\varepsilon^s_{t+1}+\varepsilon^d_{t+1}-\tau\left(b_{42}\varepsilon^z_{t+1}+b_{43}\varepsilon^d_{t+1}+b_{44}\varepsilon^m_{t+1}+b_{45}\varepsilon^s_{t+1}+b_{46}\varepsilon^a_{t+1}+\varepsilon^z_{t+1}\right)-\varepsilon^a_{t+1}+\alpha\left(b_{12}\varepsilon^z_{t+1}+b_{13}\varepsilon^d_{t+1}+b_{14}\varepsilon^m_{t+1}+b_{15}\varepsilon^s_{t+1}+b_{16}\varepsilon^a_{t+1}\right)}\right] \\
&= e^{\frac{1}{2}\left((\alpha b_{13}-\tau b_{43}+1)^2\sigma_d^2+(\alpha b_{12}-\tau b_{42})^2\sigma_z^2+(\alpha b_{14}-\tau b_{44})^2\sigma_m^2+(\alpha b_{15}-\tau b_{45}+1)^2\sigma_s^2+(\alpha b_{16}-\tau b_{46}-1)^2\sigma_a^2\right)}.
\end{aligned}$$

So, the expectation term becomes:

$$\begin{aligned}
&\mathbb{E}_t\left[(1-\delta e^{s_{t+1}})e^{\varepsilon^d_{t+1}-\tau\left(B_2^n\varepsilon_{t+1}+\varepsilon^z_{t+1}\right)-\varepsilon^a_{t+1}+\alpha B_2^\theta\varepsilon_{t+1}}\right] \\
&= \left(e^{\frac{1}{2}(\alpha b_{15}-\tau b_{45})^2\sigma_s^2}-\delta e^{\rho_s s_t+\frac{1}{2}(\alpha b_{15}-\tau b_{45}+1)^2\sigma_s^2}\right) \\
&\quad\cdot e^{\frac{1}{2}\left((\alpha b_{13}-\tau b_{43}+1)^2\sigma_d^2+(\alpha b_{12}-\tau b_{42})^2\sigma_z^2+(\alpha b_{14}-\tau b_{44})^2\sigma_m^2+(\alpha b_{15}-\tau b_{45}+1)^2\sigma_s^2+(\alpha b_{16}-\tau b_{46}-1)^2\sigma_a^2\right)}.
\end{aligned}$$

Law of motion for employment Taking the law of motion for employment and substituting the expressions for the policies yields:

$$\begin{aligned}
&e^{b_{40}+(b_{41}-1)n_{t-1}+b_{42}z_t+b_{43}d_t+b_{44}m_t+b_{45}s_t+b_{46}a_t} = \\
&1-\delta e^{s_t}+Q\theta e^{a_t+(1-\alpha)(b_{10}+b_{11}n_{t-1}+b_{12}z_t+b_{13}d_t+b_{14}m_t+b_{15}s_t+b_{16}a_t)}\left(\frac{e^{-n_{t-1}}}{N}-1+\delta e^{s_t}\right).
\end{aligned}$$

E Stochastic Growth Model with Alternative Stochastic Processes

We illustrate how to accommodate two alternative stochastic processes within our methodology: (i) stochastic volatility and (ii) regime-switching.

E.1 Basic stochastic growth model

To simplify exposition, we work through a small example: the stochastic growth model. For any exogenous driving process for total factor productivity, the equilibrium for this model can be summarized as:

$$\begin{aligned} C_t^{-\tau} &= \beta \mathbb{E}_t \left[C_{t+1}^{-\tau} \left(\alpha e^{z_{t+1}} K_{t+1}^{\alpha-1} + 1 - \delta \right) \right] \\ K_{t+1} &= e^{z_t} K_t^{\alpha} + (1-\delta) K_t - C_t. \end{aligned}$$

In a deterministic steady state, $z = 0$, and the solution is:

$$K = \left[\frac{1}{\alpha} \left(\frac{1}{\beta} - 1 + \delta \right) \right]^{\frac{1}{\alpha - 1}}, \quad C = K^{\alpha} - \delta K.$$

In what follows we consider log deviations from steady state value $c_t = \log(C_t/C)$ and $k_t = \log(K_t/K)$, so that $C_t = Ce^{c_t}$ and $K_t = Ke^{k_t}$. Substitution of this change of variables into the equilibrium gives:

$$\begin{aligned} e^{-\tau c_t} &= \mathbb{E}_t \left[e^{-\tau c_{t+1}} \left\{ \left(1 - \beta(1-\delta) \right) e^{z_{t+1} + (\alpha-1)k_{t+1}} + \beta(1-\delta) \right\} \right] \\ e^{k_{t+1}} &= \frac{1}{\alpha} \left(\frac{1}{\beta} - (1-\delta) \right) e^{z_t + \alpha k_t} + (1-\delta) e^{k_t} - \left(\frac{1}{\alpha} \left(\frac{1}{\beta} - (1-\delta) \right) - \delta \right) e^{c_t}. \end{aligned}$$

E.2 Stochastic Volatility

Stochastic volatility models introduce an exogenous shock process that no longer maps into a VAR structure as in Equation (2). While (dynamic) Taylor projection methods remain applicable, as discussed below, the filtering procedure must be adapted. A key advantage of dynamic Taylor projection in this setting is that time-varying risk directly influences the policy functions, as the solution is not certainty equivalent. By contrast, under perturbation methods, such effects require at least a fourth- or sixth-order expansion for the variance of volatility shocks to enter the decision rules (De Groot, 2016).

Consider the standard stochastic growth model augmented with a stochastic volatility (SV) shock. Productivity z_t follows an AR(1) process with SV:

$$\begin{aligned} z_t &= \rho_z z_{t-1} + e^{\xi_t/2} u_t, \\ \xi_t &= (1-\rho_\xi)\mu_\xi + \rho_\xi \xi_{t-1} + \sigma_\xi v_t. \end{aligned}$$

The state vector x_t contains capital k_t, productivity z_t, and volatility ξ_t. Assume the policy rules for consumption and capital accumulation take the form:

$$\begin{aligned} c_t &= a_0 + a_1 k_t + a_2 z_t + a_3 \xi_t, \\ k_{t+1} &= b_0 + b_1 k_t + b_2 z_t + b_3 \xi_t. \end{aligned}$$

Expectations Returning to the previous expectation terms in the Euler equation, we have the first term:

$$\begin{aligned} &\mathbb{E}_t\left[e^{-\tau c_{t+1} + z_{t+1} + (\alpha-1)k_{t+1}}\right] = \mathbb{E}_t\left[e^{-\tau(a_0 + a_1 k_{t+1} + a_2 z_{t+1} + a_3 \xi_{t+1}) + z_{t+1} + (\alpha-1)k_{t+1}}\right] \\ &= e^{-\tau(a_0 + a_1 k_{t+1}) + (\alpha-1)k_{t+1}} \mathbb{E}_t\left[e^{-\tau(a_2 z_{t+1} + a_3 \xi_{t+1}) + z_{t+1}}\right] \\ &= e^{-\tau(a_0 + a_1 k_{t+1}) + (\alpha-1)k_{t+1}} \mathbb{E}_t\left[e^{-\tau\left\{a_2\left(\rho_z z_t + e^{\xi_{t+1}/2} u_{t+1}\right) + a_3\left((1-\rho_\xi)\mu_\xi + \rho_\xi \xi_t + \sigma_\xi v_{t+1}\right)\right\} + \rho_z z_t + e^{\xi_{t+1}/2} u_{t+1}}\right]. \end{aligned}$$

Since k_{t+1} is known at time t, it can be factored out of the expectation. The relevant expectation thus reduces to:

$$\begin{aligned} &\mathbb{E}_t\left[e^{-\tau\left\{a_2\left(\rho_z z_t + e^{\xi_{t+1}/2} u_{t+1}\right) + a_3\left((1-\rho_\xi)\mu_\xi + \rho_\xi \xi_t + \sigma_\xi v_{t+1}\right)\right\} + \rho_z z_t + e^{\xi_{t+1}/2} u_{t+1}}\right] \\ &= e^{(1-\tau a_2)\rho_z z_t - \tau a_3\left((1-\rho_\xi)\mu_\xi + \rho_\xi \xi_t\right)} \mathbb{E}_t\left[\exp\left\{(1-\tau a_2) e^{\frac{(1-\rho_\xi)\mu_\xi + \rho_\xi \xi_t + \sigma_\xi v_{t+1}}{2}} u_{t+1} - \tau a_3 \sigma_\xi v_{t+1}\right\}\right]. \end{aligned}$$

Terms known at time t can be factored out of the expectation. The remaining expression involves an expectation over v_{t+1} and u_{t+1}, which can be evaluated by applying the law of iterated expectations. Conditional on v_{t+1}, the expectation over

Gaussian u_{t+1} can be computed analytically:

$$\begin{aligned}
&\mathbb{E}_t\left[\exp\left\{(1-\tau a_2)e^{\frac{(1-\rho_\xi)\mu_\xi+\rho_\xi\xi_t+\sigma_\xi v_{t+1}}{2}}u_{t+1}-\tau a_3\sigma_\xi v_{t+1}\right\}\right]\\
&=\mathbb{E}_{v_{t+1}}\left[\mathbb{E}_{u_{t+1}}\left[\exp\left\{(1-\tau a_2)e^{\frac{(1-\rho_\xi)\mu_\xi+\rho_\xi\xi_t+\sigma_\xi v_{t+1}}{2}}u_{t+1}-\tau a_3\sigma_\xi v_{t+1}\right\}\middle| v_{t+1}\right]\right]\\
&=\mathbb{E}_{v_{t+1}}\left[e^{-\tau a_3\sigma_\xi v_{t+1}}\mathbb{E}_{u_{t+1}}\left[\exp\left\{(1-\tau a_2)e^{\frac{(1-\rho_\xi)\mu_\xi+\rho_\xi\xi_t+\sigma_\xi v_{t+1}}{2}}u_{t+1}\right\}\middle| v_{t+1}\right]\right]\\
&=\mathbb{E}_{v_{t+1}}\left[\exp\{-\tau a_3\sigma_\xi v_{t+1}\}\exp\left\{\frac{(1-\tau a_2)^2}{2}e^{(1-\rho_\xi)\mu_\xi+\rho_\xi\xi_t+\sigma_\xi v_{t+1}}\right\}\right]\\
&=\mathbb{E}_{v_{t+1}}\left[\exp\left\{-\tau a_3\sigma_\xi v_{t+1}+\frac{(1-\tau a_2)^2}{2}e^{(1-\rho_\xi)\mu_\xi+\rho_\xi\xi_t+\sigma_\xi v_{t+1}}\right\}\right]\\
&=\frac{1}{\sqrt{2\pi}}\int_\infty^\infty\exp\left\{-\tau a_3\sigma_\xi v_{t+1}+\frac{(1-\tau a_2)^2}{2}e^{(1-\rho_\xi)\mu_\xi+\rho_\xi\xi_t+\sigma_\xi v_{t+1}}\right\}e^{-\frac{v_{t+1}^2}{2}}dv_{t+1}.
\end{aligned}$$

Although the expression does not admit a closed-form solution, it can be accurately approximated using Gauss-Hermite quadrature over v_{t+1}, yielding:

$$\sum_{i=1}^{N}\exp\left\{-\tau a_3\sigma_\xi v_i+\frac{(1-\tau a_2)^2}{2}e^{(1-\rho_\xi)\mu_\xi+\rho_\xi\xi_t+\sigma_\xi v_i}\right\}\omega_i,$$

where $\{v_i,\omega_i\}_{i=1}^N$ denote the nodes and weights of the Gauss-Hermite quadrature. The second expectation term is:

$$\begin{aligned}
\mathbb{E}_t\left[e^{-\tau c_{t+1}}\right]&=\mathbb{E}_t\left[e^{-\tau(a_0+a_1k_{t+1}+a_2z_{t+1}+a_3\xi_{t+1})}\right]\\
&=e^{-\tau(a_0+a_1k_{t+1})}\mathbb{E}_t\left[e^{-\tau(a_2z_{t+1}+a_3\xi_{t+1})}\right]\\
&=e^{-\tau(a_0+a_1k_{t+1}+a_2\rho_z z_t+a_3[(1-\rho_\xi)\mu_\xi+\rho_\xi\xi_t])}\mathbb{E}_t\left[e^{-\tau a_2e^{\xi_{t+1}/2}u_{t+1}-\tau a_3\sigma_\xi v_{t+1}}\right].
\end{aligned}$$

Applying iterated expectations as above:

$$\mathbb{E}_t\left[\exp\left\{-\tau a_2e^{\xi_{t+1}/2}u_{t+1}-\tau a_3\sigma_\xi v_{t+1}\right\}\right]=\mathbb{E}_{v_{t+1}}\left[\left\{\frac{(\tau a_2)^2}{2}e^{(1-\rho_\xi)\mu_\xi+\rho_\xi\xi_t+\sigma_\xi v_{t+1}}-\tau a_3\sigma_\xi v_{t+1}\right\}\right],$$

which can be approximated by:

$$\sum_{i=1}^{N}\exp\left\{\frac{(\tau a_2)^2}{2}e^{(1-\rho_\xi)\mu_\xi+\rho_\xi\xi_t+\sigma_\xi v_i}-\tau a_3\sigma_\xi v_i\right\}\omega_i.$$

State Space Form Assume we observe both output, given by $y_t = z_t + \alpha k_t$, and consumption. In that case, we obtain a measurement equation:

$$\begin{bmatrix} y_t \\ c_t \end{bmatrix} = \begin{bmatrix} 0 \\ a_0 \end{bmatrix} + \begin{bmatrix} \alpha & 1 & 0 \\ a_1 & a_2 & a_3 \end{bmatrix} \begin{bmatrix} k_t \\ z_t \\ \xi_t \end{bmatrix} + \varepsilon_t, \quad \varepsilon_t \sim N(0, H),$$

with H measurement error variance. Labeling $x_t = (k_t,\ z_t,\ \xi_t)'$, and $\eta_t = (u_t,\ v_t)'$, the state transition equation of the form:

$$x_t = \begin{bmatrix} b_0 \\ 0 \\ (1-\rho_\xi)\mu_\xi \end{bmatrix} + \begin{bmatrix} b_1 & b_2 & b_3 \\ 0 & \rho_z & 0 \\ 0 & 0 & \rho_\xi \end{bmatrix} x_{t-1} + \underbrace{\begin{bmatrix} 0 & 0 \\ e^{\xi_t} & 0 \\ 0 & 1 \end{bmatrix}}_{R(\xi_t)} \eta_t, \quad \eta_t \sim N(0, \mathrm{diag}(\sigma_u, \sigma_v)^2).$$

Filtering The only deviation from our baseline filtering framework is that $R(\xi_t)$ is now a nonlinear function of the volatility state. A simple approach is to apply the Extended Kalman Filter (EKF), which replaces $R(\xi_t)$ with $R(\hat{\xi}_{t|t-1})$, a zeroth-order Taylor approximation around the predicted state. That is, e^{ξ_t} in $R(\xi_t)$ is approximated by $e^{\hat{\xi}_{t|t-1}}$. Note that the observables directly load on volatility, which identifies the system. An alternative is to discretize the stochastic process for ξ_t using a finite-state Markov chain, as in Friedman and Harris (1998), with the method of Tauchen (1986). Conditional on ξ_t, the model is linear and Gaussian, and the likelihood can be evaluated using the filter of Hamilton (1994). This approach is not discussed further, as it is subsumed by the regime-switching specification considered below.

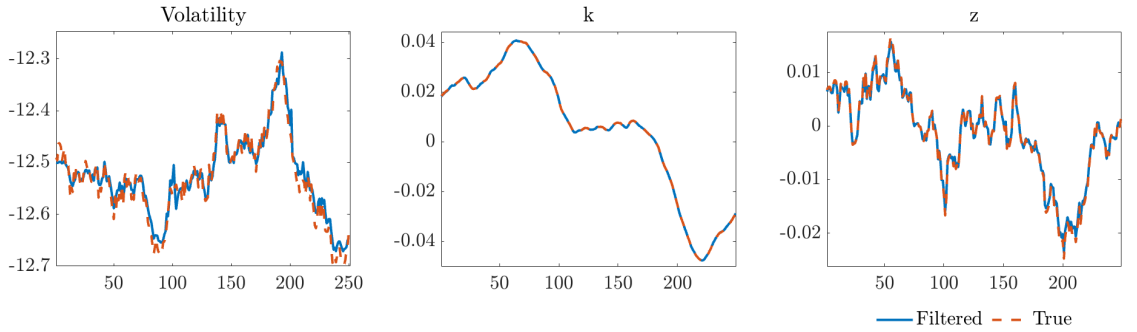
Parameters We use $\rho_z = 0.95$, $\mu_\xi = -12.5$, $\rho_\xi = 0.975$, $\sigma_\xi = 0.02$ for the exogenous process. For the economic parameters, we set risk aversion to 6, $\beta = 1.04^{-1/4}$, $\alpha = 0.36$ and $\delta = 0.05$.

Demonstration Figure E1 compares the performance of the two filters using simulated data on output and consumption of length $T = 250$. For the discretization-based filter, we apply the Tauchen method with 250 grid points. We assume in the simulation that consumption is measured with a noise level of 0.01% of the

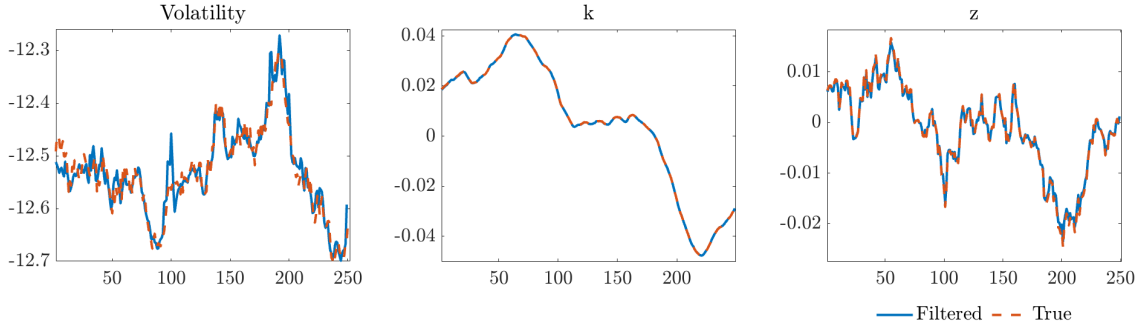
standard deviation, and output with measurement error 0.05% of the standard deviation. As the figure shows, both filters track volatility, capital and TFP closely.

Figure E1: Filtered States and Fitted Values

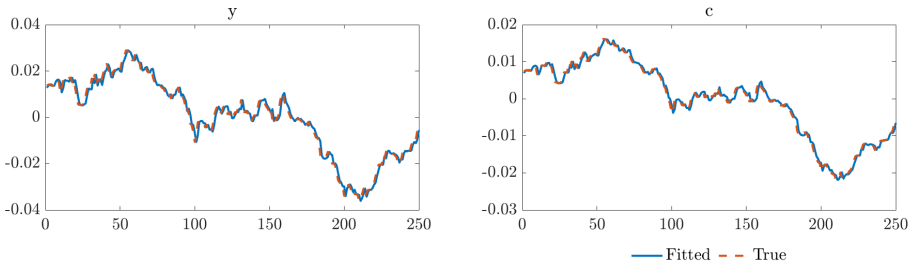
(a) Filtered States: Extended Kalman filter



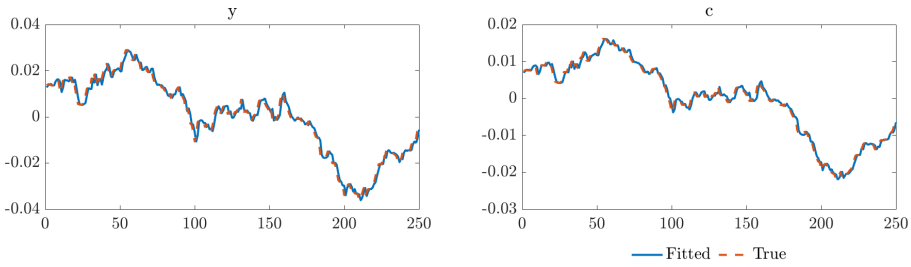
(b) Filtered States: Discretized volatility following Friedman and Harris (1998)



(c) Fitted Values: Extended Kalman filter



(d) Fitted Values: Discretized volatility following Friedman and Harris (1998)



E.3 Regime Switching

A common extension in macroeconomic models allows exogenous state dynamics to follow a regime-switching process. This class includes models with rare disasters and other forms of time-varying volatility. Specifically, let $s_t \in \{0, 1\}$ denote a latent regime indicator that evolves according to the transition matrix

$$s_t \sim \Pi, \qquad \Pi = \begin{bmatrix} p_0 & 1 - p_0 \\ 1 - p_1 & p_1 \end{bmatrix},$$

where $p(s_{t+1} = 1 \mid s_t = 1) = p_1$ and $p(s_{t+1} = 0 \mid s_t = 0) = p_0$. Although the framework extends naturally to multiple regimes, we focus on the two-state case for exposition. The latent state s_t governs the evolution of productivity z_t:

$$z_{t+1} = \begin{cases} \rho_0 z_t + \sigma_0 \eta_{t+1} & \text{if } s_t = 0, \\ \rho_1 z_t + \sigma_1 \eta_{t+1} & \text{if } s_t = 1, \end{cases} \qquad \eta_t \sim N(0, 1). \tag{E.1}$$

As before, let $y_t = z_t + \alpha k_t$, and define the state vector as $x_t = (k_t, z_t)$. The policy function for consumption and the law of motion for capital are regime-dependent as denoted by:

$$\begin{aligned} c_t &= a_{j0} + a_{j1} k_t + a_{j2} z_t, \\ k_{t+1} &= b_{j0} + b_{j1} k_t + b_{j2} z_t \end{aligned}$$

so the coefficient vectors $\mathbf{a}_j$ and $\mathbf{b}_j$ are assumed to vary with the regime $j = s_t$.

Expectations The regime-switching policy rules imply that the realization of consumption at time $t + 1$ depends on the state sequence s_t, s_{t+1}:

$$c_{t+1} = \Big\{ a_{j0} + a_{j1} b_{i0} + a_{j1} b_{i1} k_t + (a_{j1} b_{i2} + a_{j2} \rho_j) z_t + a_{j2} \sigma_j \eta_{t+1}, \text{ if } s_t = i, s_{t+1} = j$$

Using iterated expectations, the expectation terms in the Markov model can be written as:

$$\mathbb{E}_t[\cdot] = \mathbb{E}_{s_{t+1}}[\mathbb{E}_{z_{t+1}}[\cdot | s_{t+1}, s_t, z_t] | s_t].$$

Applying this to the first expectation term in the Euler equation yields:

$$\mathbb{E}_{z_{t+1}}\left[e^{-\tau c_{t+1}+z_{t+1}+(\alpha-1)k_{t+1}}|s_{t+1}, s_t, z_t\right] =$$
$$\exp\left\{-\tau(a_{j0}+a_{j1}b_{i0}+a_{j1}b_{i1}k_t+(a_{j1}b_{i2}+a_{j2}\rho_j)z_t)+\rho_j z_t+(\alpha-1)k_{t+1}+\frac{(1-\tau a_{j2})^2\sigma_j^2}{2}\right\},$$

if $s_t = i$ and $s_{t+1} = j$. Here, k_{t+1} is determined by s_t and other known variables at time t. Similarly,

$$\mathbb{E}_{z_{t+1}}\left[e^{-\tau c_{t+1}}\right] = \exp\left\{-\tau(a_{j0}+a_{j1}b_{i0}+a_{j1}b_{i1}k_t+(a_{j1}b_{i2}+a_{j2}\rho_j)z_t)+\frac{(\tau a_{j2})^2\sigma_j^2}{2}\right\}.$$

These expressions show that the regime-switching model also allows expectations to be evaluated analytically under the Taylor projection approach, without numerical integration.

State Space Representation Conditional on s_t, this is simply a linear state space system, with, for $s_t = j$, a measurement equation

$$\begin{bmatrix} y_t \\ c_t \end{bmatrix} = \begin{bmatrix} 0 \\ a_{j0} \end{bmatrix} + \begin{bmatrix} \alpha & 1 \\ a_{j1} & a_{j2} \end{bmatrix} \begin{bmatrix} k_t \\ z_t \end{bmatrix} + \varepsilon_t, \quad \varepsilon_t \sim N(0, H).$$

and, again for $s_t = j$, the state transition equation is given by

$$\begin{bmatrix} k_{t+1} \\ z_{t+1} \end{bmatrix} = \begin{bmatrix} b_{j0} \\ 0 \end{bmatrix} + \begin{bmatrix} b_{j1} & b_{j2} \\ 0 & \rho_j \end{bmatrix} \begin{bmatrix} k_t \\ z_t \end{bmatrix} + \begin{bmatrix} 0 \\ \sigma_j \end{bmatrix} \eta_t, \quad \eta_t \sim N(0,1).$$

Filter To initialize the filter, set $x_{1|0}$, $P_{1|0}$, and $\hat{\xi}_{1|0}$, where $\hat{\xi}_{1|0}$ contains the regime probabilities $\mathbb{P}(s_1 = j)$ prior to observing any data. These can, for example, be initialized using the stationary distribution implied by Π. Solve the model at $x_{1|0}$ using Taylor projection. Then, for each regime $j \in \{0, 1\}$, perform the update and prediction steps of Algorithm 1.

For each regime, compute the regime-specific likelihood contribution $\ell_t^{(j)}$ by evaluating the forecast error v_t under a normal distribution with mean zero and variance

F_t. The regime probabilities are then updated as:

$$\hat{\xi}_{t|t}^{(j)} := \mathbb{P}(s_t = j \mid y_{1:t}^{\text{obs}}) = \frac{\ell_t^{(j)} \cdot \hat{\xi}_{t|t-1}^{(j)}}{\sum_{j'=0}^{1} \ell_t^{(j')} \cdot \hat{\xi}_{t|t-1}^{(j')}}, \quad j \in \{0, 1\}.$$

Following Hamilton (1994), the predicted regime probabilities are:

$$\hat{\xi}_{t|t-1} = \Pi \cdot \hat{\xi}_{t-1|t-1},$$

where $\hat{\xi}_{t-1|t-1}^{(i)} = \mathbb{P}(s_{t-1} = i \mid y_{1:t-1}^{\text{obs}})$ is the filtered probability from the previous period, and $\hat{\xi}_{t|t-1}^{(i)}$ is the forecasted probability of regime i at time t.

Latent variables are then filtered and forecasted via regime-weighted averages. For instance:

$$\hat{z}_{t|t} = \sum_{j=0}^{1} \hat{\xi}_{t|t}^{(j)} \cdot \hat{z}_{t|t}^{(j)}, \quad \hat{z}_{t+1|t} = \sum_{j=0}^{1} \hat{\xi}_{t+1|t}^{(j)} \cdot \hat{z}_{t+1|t}^{(j)},$$

where $\hat{z}_{t|t}^{(j)}$ denotes the filtered state conditional on regime j. The model is then re-solved using Taylor projection at $\hat{x}_{t+1|t}$, and the Kalman update and prediction steps are repeated.

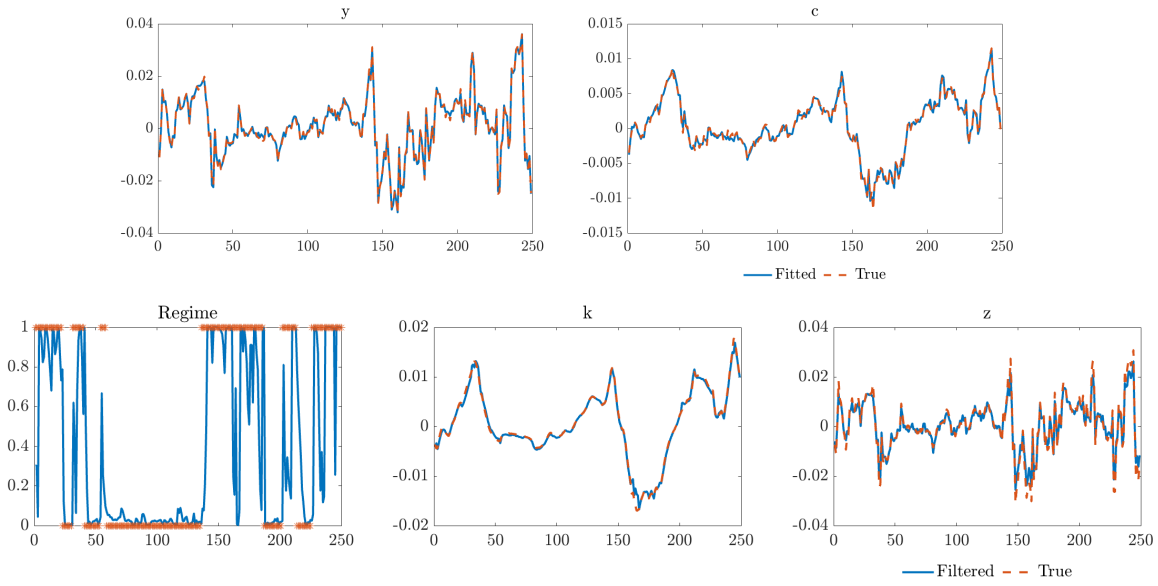
Parameters We use the following parameterization: $p_0 = 0.97$, $\rho_0 = 0.8$, $\sigma_0 = 0.01$, $p_1 = 0.95$, $\rho_1 = 0.95$, $\sigma_1 = 0.002$, risk aversion $\tau = 2$, $\beta = 1.04^{-1/4}$, $\alpha = 0.36$ and $\delta = 0.025$.

Demonstration To illustrate the performance of the filter described above, we simulate a dataset of length $T = 250$ from the dynamic Taylor Projection model solution. We assume measurement error is 10% of the standard deviation of the observed data in the simulation below. We then recover the latent states using the filter. Results are visualized in Figure E2. As we can see in this figure, the filtered states track the true values used in the simulation closely. It takes about 1.3 seconds to run the filter 100 times on a dataset of length $T = 250$.

F Heterogeneous Agent Models

Equilibrium The aggregate states of the model are $x_t = (z_t, \mu_t)$, with μ_t the distribution of households over employment and assets, i.e., (ε, a). The equilibrium

Figure E2: Fitted values (top) and filtered and true states values (bottom)



unknowns are next period's assets, $a'(\varepsilon, a; z, \mu)$, interest rate $r(z, \mu)$, wages $w(z, \mu)$ and distribution $\mu'(z, \mu)$, which have to satisfy three sets of conditions:

1. For given prices and law of motion of the distribution, household optimization satisfies: $c(\varepsilon, a; z, \mu)^{-\sigma} \geq \beta \mathbb{E}\left[(1 + r(z', \mu'(z, \mu)))c(\varepsilon', a'(\varepsilon, a; z, \mu); z', \mu'(z, \mu))^{-\sigma} | \varepsilon, z, \mu\right]$ with equality if $a'(\varepsilon, a; z, \mu) \geq 0$. Here $c(\varepsilon, a; z, \mu) = w(z, \mu)((1 - \tau)\varepsilon + b(1 - \varepsilon)) + (1 + r(z, \mu))a - a'(\varepsilon, a; z, \mu)$ is optimal consumption.

2. Interest rate and wages satisfy:

$$r(z, \mu) = \alpha e^z K^{\alpha - 1} L^{1-\alpha} - \delta$$
$$w(z, \mu) = (1 - \alpha) e^z K^{\alpha} L^{-\alpha}$$

   where $K = \sum_{\varepsilon} \int a d\mu(\varepsilon, a)$.

3. Law of motion for the distribution: for all measurable sets Λ_a,

$$\mu'(z, \mu)(\varepsilon, \Lambda_a) = \sum_{\tilde{\varepsilon}} \pi(\varepsilon | \tilde{\varepsilon}, z) \int 1\{a'(\tilde{\varepsilon}, a; z, \mu) \in \Lambda_a\} \mu(\tilde{\varepsilon}, da)$$

Computation The state space representation closely follows Winberry (2018). After dimension-reduction, the model has six states: $x_t = \left(z_t, m^1_{0t}, m^2_{0t}, m^1_{1t}, m^2_{1t}, L_t\right)'$. These include aggregate productivity z_t; the first and second moments of the wealth

distribution for unemployed households, (m_{0t}^1, m_{0t}^2); the first and second moments for employed households, (m_{1t}^1, m_{1t}^2); and aggregate employment L_t. The model also includes 24 control variables:

$$y_t = \left(\theta_{0,t}^1, \ldots, \theta_{0,t}^9, \theta_{1,t}^1, \ldots, \theta_{1,t}^9, g_{0,t}^0, g_{0,t}^1, g_{0,t}^2, g_{1,t}^0, g_{1,t}^1, g_{1,t}^2\right)'.$$

Here, $\theta_{\varepsilon,t}^j$ for $j = 1, \ldots, 9$ are the Chebyshev coefficients used to approximate the continuation value, and $g_{\varepsilon,t}^k$ for $k = 0, 1, 2$ are the coefficients that parametrize the density function of wealth for each employment status.

We approximate the moments using $n_\ell = 15$ Gauss–Legendre nodes and weights $\{a_\ell, \omega_\ell\}_{\ell=1}^{n_\ell}$, where the implied density at each node is given by:

$$h_{\varepsilon,t}^\ell = \exp\left(g_{\varepsilon,t}^0 + g_{\varepsilon,t}^1 a_\ell + g_{\varepsilon,t}^2 a_\ell^2\right)\omega_\ell.$$

We also use $n_\psi = 9$ Chebyshev nodes $\{a_i\}_{i=1}^{n_\psi}$ to approximate the unconstrained expected marginal utility.

We can write the approximate equilibrium conditions compactly as:

$$\mathbb{E}_t\left[f\left(y_t, y_{t+1}, x_t, x_{t+1}\right)\right] =$$

$$\mathbb{E}_t\begin{bmatrix} z_{t+1} - \rho_z z_t - \sigma_e \eta_{t+1} \\ m_{\varepsilon,t+1}^k - \frac{p(\varepsilon|0,z_t)(1-L_t)\sum_\ell \{a_{t+1}(0,a_\ell)\}^k h_{0,t}^\ell + p(\varepsilon|1,z_t)L_t \sum_\ell \{a_{t+1}(1,a_\ell)\}^k h_{1,t}^\ell}{\varepsilon L_{t+1} + (1-\varepsilon)(1-L_{t+1})} \\ \exp\left\{\sum_{j=1}^{n_\psi} \theta_{\varepsilon,t}^j T_{j-1}(\xi(a_i))\right\} - \beta(1+r_{t+1})\sum_{\varepsilon_{t+1}} p(\varepsilon_{t+1}|\varepsilon, z_t) c_{t+1}\left(\varepsilon_{t+1}, a_{t+1}(\varepsilon, a_i)\right)^{-\sigma} \\ 1 - \sum_\ell h_{\varepsilon,t}^\ell \\ m_{\varepsilon,t}^k - \sum_\ell \{a_\ell\}^k h_{\varepsilon,t}^\ell \\ L_{t+1} - f_t(1-L_t) - (1-s_t)L_t \end{bmatrix},$$

for $k = 1, 2$ moments, $\varepsilon = 0, 1$ employment states, and $i = 1, \ldots, 9$ asset grid points, leading to $30 = \dim(x_t) + \dim(y_t)$ total equilibrium conditions. For the Taylor Projection solution we define $R(x_t, \Theta) = \mathbb{E}_t\left[f\left(y_t, y_{t+1}, x_t, x_{t+1}; \Theta\right)\right]$ using the equations described in the main text.

Parameters The discount factor is set to $\beta = 0.96$, and the inverse IES is $\sigma = 1$. Unemployment benefits are set to $b = 0.15$. The steady-state separation and job-finding probabilities are set to $\bar{s} = 0.038$ and $\bar{f} = 0.5$, respectively. The elasticities of the job-finding and separation rates with respect to aggregate productivity z_t are $\eta_f = 15$ and $\eta_s = -9$. The production function features a capital share of $\alpha = 0.36$ and a depreciation rate of $\delta = 0.10$. TFP follows an AR(1) process with persistence $\rho_z = 0.859$ and innovation standard deviation $\sigma_z = 0.01$.

Asymmetry Figure F1 plots the responses of aggregate variables to a ±1 standard deviation productivity shock at the steady state $x_t = \bar{x}$, expressed as log deviations from steady-state values. Because the perturbation solution is linear in levels, the log transformation introduces mild asymmetries. In contrast, the dynamic Taylor projection solution produces more pronounced asymmetries across all aggregates. To aid visual comparison, the response to a positive shock is multiplied by minus one. For variables such as output, employment, and consumption, asymmetries show up through magnitude. For other variables, such as investment, they affect the shape: investment exhibits a hump-shaped response to negative shocks that is absent following a positive shock. This notable asymmetry is not captured by the perturbation solution.

Figure F1: Asymmetry in a Heterogeneous Household Model: Perturbation versus Dynamic Taylor Projection, response to a one-standard deviation change in z_t.

